Int J Appl Earth Obs Geoinformation 61 (2017) 55–69

Contents lists available at ScienceDirect

Int J Appl Earth Obs Geoinformation

journal homepage: www.elsevier.com/locate/jag

Multi-Data Approach for remote sensing-based regional crop rotation mapping: A case study for the Rur catchment, Germany

Guido Waldhoff*, Ulrike Lussem, Georg Bareth

Institute of Geography, University of Cologne, Albertus-Magnus-Platz, 50923 Cologne, Germany

ARTICLE INFO

Keywords:
Crop rotation
Regional agro-ecosystem modeling
Crop classification
Phenology
GIS
Ancillary data

ABSTRACT

Spatial land use information is one of the key input parameters for regional agro-ecosystem modeling. Furthermore, to assess the crop-specific management in a spatio-temporal context accurately, parcel-related crop rotation information is additionally needed. Such data is scarcely available for a regional scale, so that only modeled crop rotations can be incorporated instead. However, the spectrum of the occurring multiannual land use patterns on arable land remains unknown. Thus, this contribution focuses on the mapping of the actually practiced crop rotations in the Rur catchment, located in the western part of Germany. We addressed this by combining multitemporal multispectral remote sensing data, ancillary information and expert-knowledge on crop phenology in a GIS-based Multi-Data Approach (MDA). At first, a methodology for the enhanced differentiation of the major crop types on an annual basis was developed. Key aspects are (i) the usage of physical block data to separate arable land from other land use types, (ii) the classification of remote sensing scenes of specific time periods, which are most favorable for the differentiation of certain crop types, and (iii) the combination of the multitemporal classification results in a sequential analysis strategy. Annual crop maps of eight consecutive years (2008–2015) were combined to a crop sequence dataset to have a profound data basis for the mapping of crop rotations. In most years, the remote sensing data basis was highly fragmented. Nevertheless, our method enabled satisfying crop mapping results. As an example for the annual crop mapping workflow, the procedure and the result of 2015 are illustrated. For the generation of the crop sequence dataset, the eight annual crop maps were geometrically smoothened and integrated into a single vector data layer. The resulting dataset informs about the occurring crop sequence for individual areas on arable land, so that crop rotation schemes can be derived. The resulting dataset reveals that the spectrum of the practiced crop rotations is extremely heterogeneous and contains a large amount of crop sequences, which strongly diverge from model crop rotations. Consequently, the integration of remote sensing-based crop rotation data can considerably reduce uncertainties regarding the management in regional agro-ecosystem modeling. Finally, the developed methods and the results are discussed in detail.

1. Introduction

In the context of food security and climate change studies, the optimized management of crops, the forecasting of crop yield, and the modeling of matter fluxes in agro-ecosystems becomes more important (Mulla, 2013; Teluguntla et al., 2015; Thenkabail, 2010). Nowadays, the impact of management strategies on crop yield can be simulated with regional agro-ecosystem models (Giltrap et al., 2010; Resop et al., 2012; Schneider, 2003; van Wart et al., 2013). These models require a large number of input parameters on soil and management properties as well as spatial weather data in a high temporal resolution (Bareth, 2009). One of the key input data for regional agro-ecosystem modeling are spatial land use data including the information on crop types and crop rotations. The latter are of key importance to determine the crop-specific management in a spatio-temporal context within the models (Giltrap et al., 2010; Kersebaum et al., 2007; Lenz-Wiedemann et al., 2010; Lobell et al., 2015; Nendel et al., 2011; Wilson and Al-Kaisi, 2008). However, spatio-temporal data on crop types and on crop rotations at the field level for regional scales are rarely available. One of the seldom examples for the availability of multiannual crop maps are the Cropland Data Layers (CDL) for the Unites States, provided by the National Agricultural Statistics Service (NASS) of the US Department of Agriculture (Boryan et al., 2011). Based on the CDL data, also planting frequency maps for corn, soybeans, wheat, and cotton are provided (Boryan et al., 2014), but spatial data on the actual crop rotations are not included. Leteinturier et al. (2006) conducted a crop

* Corresponding author.
E-mail addresses: guido.waldhoff@uni-koeln.de (G. Waldhoff), ulrike.lussem@uni-koeln.de (U. Lussem), g.bareth@uni-koeln.de (G. Bareth).

http://dx.doi.org/10.1016/j.jag.2017.04.009
Received 27 July 2016; Received in revised form 18 April 2017; Accepted 20 April 2017
Available online 14 May 2017

sequnece analysis for the Wallon region of Belgium based on data gathered in the framework of the Integrated Administration and Control System for European Union member states. However, in most European countries, such information is not available to the general public, due to data protection laws. The lack of this information is a major drawback for regional agro-ecosystem modeling, since large uncertainties concerning the management and the site-specific matter fluxes arise (Kersebaum et al., 2007). To reduce these uncertainties, usually only a few different prototype crop rotations are considered, which are based on expert-knowledge or designed according to good farming practice (Brisson et al., 2003; Klöcking et al., 2003; Rounsevell et al., 2003; Schönhart et al., 2011). However, the degree to which these assumptions on the occurrence of crop rotations can meet reality is in question. Therefore, the overarching goals of this study are (i) to produce a crop sequence data set for the study area using multiannual crop classifications and (ii) to identify spatio-temporal patterns on the actually practiced crop rotations within the crop sequence data. A central hypothesis within the process of classifying different crop rotations is that the crop sequence data has to include at least eight consecutive years. The latter is due to the fact that crop rotations in central Europe can cover a timespan from two to five years (Castellazzi et al., 2008; Munzert, 2006).

The analysis of satellite remote sensing data is a cost-effective way to generate up-to-date crop classification maps for larger areas at various scales (Atzberger, 2013; Conrad et al., 2010; Thenkabail, 2012; Waldner et al., 2015; Wardlow et al., 2007; Wu et al., 2015). By combining the precise multiannual crop type data, a data base for the spatio-temporal identification of crop sequences and crop rotations can be built. For crop mapping on a regional scale (larger than 1000 km^2), usually multispectral remote sensing data of moderate spatial resolution (ca. 10–30 m) is still the most reasonable choice. Nevertheless, many studies also demonstrate the potential of satellite-borne synthetic aperture radar (SAR) data (Bargiel and Herrmann, 2011; Hütt et al., 2016; Koppe et al., 2013; McNairn et al., 2014) and their combination with optical data (Blaes et al., 2005; Forkuor et al., 2014; McNairn et al., 2009; Lussem et al., 2016) for land use/land cover mapping.

In any case, the generation of comprehensive crop classification maps is usually hampered by limits in the technical capabilities of remote sensing systems (e.g. spectral or radiometric resolution), with regard to high spectral similarities of certain crop types. Varying crop development (e.g. winter/summer crops) or weather conditions (Whitcraft et al., 2015) are additional aspects, which hinder the crop differentiation. These factors necessitate multitemporal observations to capture and differentiate all crop types. Nowadays, the consideration of crop phenology and multitemporal data is well established to achieve results superior to monotemporal classifications (Conrad et al., 2010; De Wit and Clevers, 2004; Foerster et al., 2012; Siachalou et al., 2015; Turker and Arikan, 2005; Waldhoff et al., 2012). For the reduction of misclassifications caused by the confusion with non-agricultural vegetation, ancillary information like topographical data (Bareth, 2001; Rohierse and Bareth, 2004) or agricultural parcel boundary data (Smith and Fuller, 2001) are additionally incorporated using GIS-methods. Such approaches are often enhanced by integrating expert-knowledge in the form of production rule-based methods (Bareth, 2008; Lucas et al., 2011; Roy et al., 2015; Waldner et al., 2015) or via decision trees (Peña-Barragán et al., 2011; Peña et al., 2014). The major advantage of integrating available GIS data sources in remote sensing classifications is the avoidance of classifying urban or non-agricultural vegetation as crop or grassland. Additionally, land use information that cannot be retrieved from remote sensing data, for instance on urban, industrial, mining, or transportation land use, can be integrated in the final land use product. Finally, other studies focus more on multi classifier set-ups (Löw et al., 2015), sophisticated state-of-the-art algorithms like random forest (Belgiu and Drăguţ, 2016; Long et al., 2013) or on the fine-tuning of training data to improve crop mapping results (Mathur and Foody, 2008).

Concerning the general multitemporal crop classification strategy, methods building upon the combined analysis of multitemporal images in a single data stack (Li et al., 2015; Wardlow et al., 2007; Zheng et al., 2015) can be differentiated from a group of various approaches, which combine analysis results of multiple remote sensing datasets in a sequential or nested fashion (De Wit and Clevers, 2004; Turker and Arikan, 2005; Van Niel and McVicar, 2004; Waldhoff et al., 2012). Incidentally, these approaches are applied in a per-pixel as well as in an object-based fashion (Blaschke, 2010). In this regard, Duro et al. (2012) or Dingle Robertson and King (2011) report that in general none of these two fundamental approaches can be considered superior to the other, when using moderate spatial resolution image data.

However, since rather large areas have to be fully covered year by year for regional studies, different framework conditions apply compared to single year studies. As a result, not all approaches may be adequate for the production of uniform crop maps of multiple years, which can be combined to provide crops sequence information at the field level, and to finally conduct crop rotation mapping at the field level. For instance, larger study areas are sometimes not entirely covered by a single remote sensing scene. This may be due to the study area size, offsets between the study area location (and the extent) and the ground pass of the remote sensor swath or, especially in temperate mid-latitude regions, due to cloud coverage (Whitcraft et al., 2015). In such cases, sufficient remote sensing data coverage can only be obtained by additionally incorporating scenes from multiple sensors, which just cover fragments of the study area. As a result, varying spatial and temporal remote sensing image coverage may lead to different preconditions for the crop identification for the individual study area fragments. Furthermore, analysis methods, which are highly adapted to specific input imagery and/or acquisition conditions may not be beneficial, if their adaption to other remote sensing data requires time consuming modifications to the algorithm (Franklin et al., 2011).

In this context, the central task of this study was the design and the application of a robust and annually reproducible crop mapping approach, which can cope with temporally and spatially fragmented remote sensing data. Besides the consideration of crop phenology, the integration of spatially precise data on agricultural land use and land cover from official data sources was a key factor to obtain the desired information. We addressed this by combining remote sensing analysis procedures and GIS-methods for the integration of ancillary information and expert knowledge on crop phenology in a Multi-Data Approach (MDA).

For the generation of a profound data base for crop rotation mapping, this MDA has been used for annual crop type mapping for eight consecutive years (2008–2015). The annual crop mapping methodology and validation of the achieved results is exemplarily illustrated in this contribution for the year 2015. The MDA concept was then extended, to combine the eight annual crop maps to a single dataset to obtain crop sequence information. Finally, with the analysis of the resulting crop sequence dataset we address the overarching question, if crop rotations can be sufficiently identified and can be used as input parameter for regional agro-ecosystem modeling of our study area.

2. Study area and crop phenology

2.1. Study area

The catchment of the river Rur is mainly situated in western Germany (North Rhine-Westphalia, NRW), but it also reaches into the Netherlands and Belgium. To include entire municipalities in Germany, the study area was slightly expanded to about 3400 km^2 in total. The available ancillary data used for the analysis differs between the countries. In this paper, the methods and results for the German part in NRW are presented.

The northern part of the study area is characterized by mainly flat

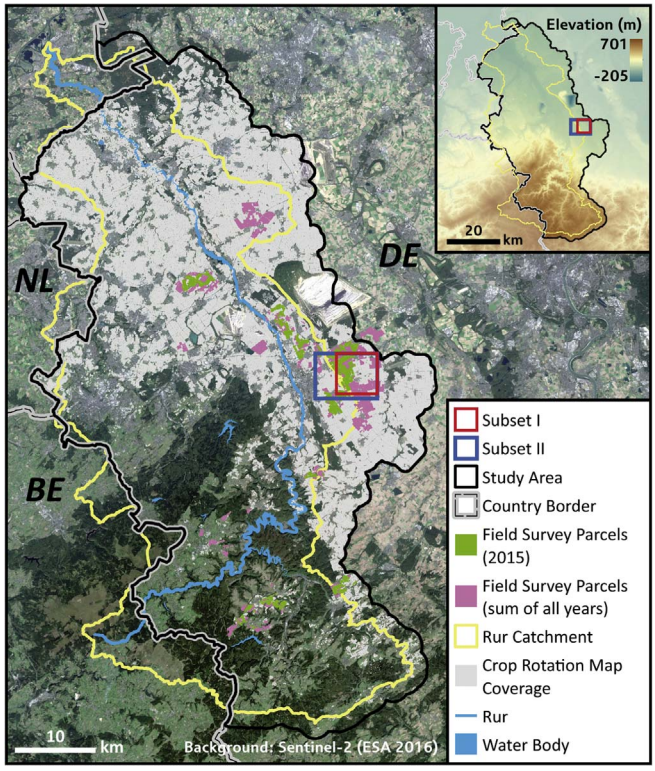

Fig. 1. Overview of the study area, the German part of the Rur catchment.

terrain with intensive agriculture, whereas the low mountain ranges of the southern part are dominated by forest areas and grass land (cf. Fig. 1). Due to change of relief toward higher elevations in the southern part, the study area can be divided into several regions with slightly differing timing of general crop development and composition of the cultivated crops. The main cultivated crops in the study area are winter wheat (WW), winter barley (WB), winter rapeseed (WR), sugar beet (SB), potato (P) and maize (M). In terms of acreage, winter wheat and sugar beet usually significantly outnumber the other crops. Within cereals, winter rye (R) was also frequently mapped in the eastern part, whereas spring barley (SPB) is of relevance in the southern part (IT.NRW, 2009).

2.2. Phenology of the dominant crops in the Rur catchment

For the differentiation of crop types with optical remote sensing data with our Multi-Data Approach, phenology is considered as a key factor (Oetter et al., 2000; Pax-Lenney and Woodcock, 1997). Therefore, a phenology model for the major crop types in the study area was created. The expansion of the bars in Fig. 2 illustrates the average presence of the different crop types on arable land in the growing season between April and September. The coloring indicates the average occurrence of significant development stages of the crop types in connection with their typical appearance in the remote sensing images from a certain acquisition period. Increasing opacity from the left end of the bars indicates (where applicable) that weather conditions, varying crop development and the individual management of the farmers (e.g. sowing dates) may induce annual or inter-parcel differences concerning the general canopy closure for a certain crop type. Likewise, decreasing opacity to the right end of the bars accounts for annual shifts or management-caused inter-parcel discrepancies regarding the disappearance (harvesting) of crops.

By reading Fig. 2 from left to right, green colors indicate the presence or the potential detectability of green vegetation on parcels with the specific crop. For cereals and rapeseed, color shifts from green to light green, to yellow and finally to orange/beige denote the approximate time periods at which the principal growth stages (Meier, 2001) flowering, fruit development, and maturity of fruits (or the transitions between them) occur. In particular, the positions of light green and yellow sections of one crop type relative to the others indicate phases favorable for the differentiation of certain crop types. For example, owing to its comparatively early (yellow) flowering, rapeseed usually is detected best from the second half of April until mid-May. At other phases, its spectral appearance is very similar to most (winter) cereals in multispectral images. Similarly, the spectral appearance of winter barley usually differs the most from winter wheat in the first half of June. This is due to the fact that winter barley already undertakes heading and flowering in this period, while winter wheat is usually still in the booting stage. In contrast, sugar beet and maize scarcely develop significant spectral characteristics that can be attributed to specific growth stages. Nevertheless, they gradually develop spectral differences, which become most visible in late July or August. In Fig. 2 this is indicated by different tones of green.

2.3. Remote sensing data acquisition planning

Based on the analysis of the phenology model presented in the previous section, several phases advantageous for an improved crop differentiation unfold. With regard to efficient remote sensing data analyses, five annual acquisition windows (AW) were selected (dashed line symbol rectangles in Fig. 2). The primary goal of each acquisition window was the direct discrimination of specific crops with the corresponding satellite images.

Table 1 outlines the time frame and the main purpose for the image acquisitions of each acquisition windows. To account for possible data gaps, for example caused by cloud coverage, some aims are defined for multiple acquisition windows.

After the image acquisition and selection was completed, each image (or associated images with similar acquisition dates) was regarded as a unique time step for the further analysis. However, in most of the years, it was not possible to obtain imagery for each of the acquisition windows. Additionally, also data outside of the acquisition windows had to be used. Thus, the numbering of the time steps was, in the end, independent from the numbering of the acquisition windows and was only intended to indicate the chronological order of the imagery.

Tables informing about the remote sensing datasets that went into the analysis in all eight years are provided in Supplement A.

3. Remote sensing data and ancillary data

The Multi-Data Approach (MDA) applied in this study is characterized by the integration of ancillary information at several phases of the analysis. Already for the remote sensing data analysis adequate ancillary data was a key factor to obtain spatial crop type information in the required detail from the available imagery. In the following, the datasets selected for the German part of the study area are described. These were used to separate arable land from other land use types and to spatially align all datasets for the MDA analysis. During the data preprocessing, all vector data were rasterized and, as well as the remote sensing data, resampled to a spatial resolution of 15 m (for the explanation, please see Section 3.3).

3.1. Authorative Topographic-Cartographic Information System (ATKIS)

The Authorative Topographic-Cartographic Information System (ATKIS) is the Digital Landscape Model (DLM) for Germany. It is provided by the official survey and mapping agencies of the federal states of Germany, in this case GeobasisNRW. The vector-based ATKIS Basis DLM (henceforth referred to as ATKIS) provides diverse topographical and land use information for example on the transport system, built-up areas, forest areas, and agricultural land at a scale of

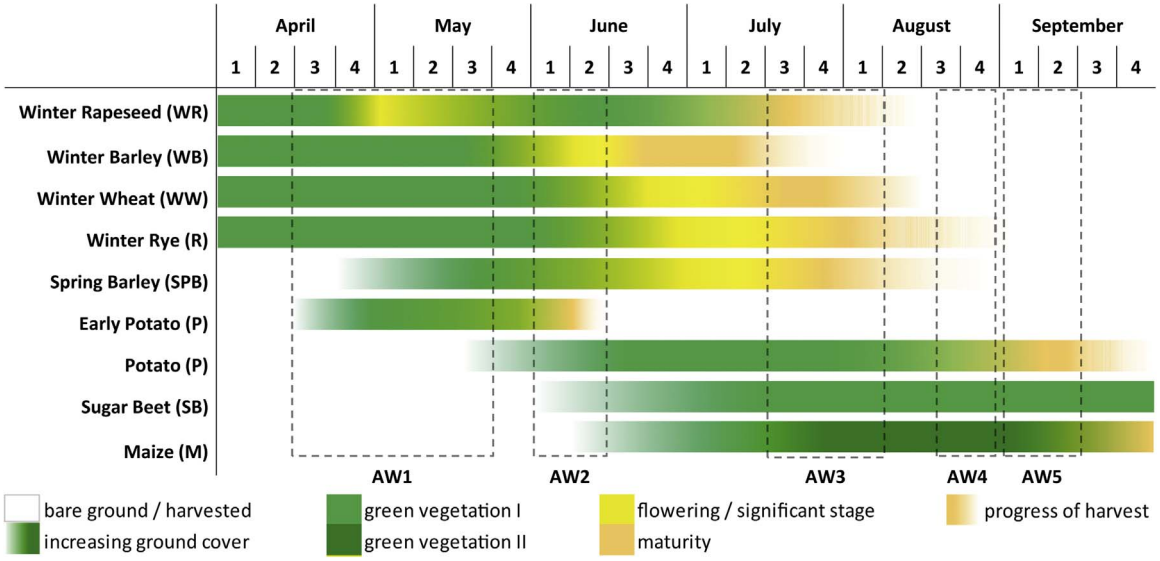

Fig. 2. Model of the phenology in conjunction with the projected detectability and discriminability of the major crop types in the Rur catchment by the analysis of multitemporal optical remote sensing data. For clarity the month are divided into four parts. Dashed line symbol rectangles delineate selected acquisition windows (AW) for remote sensing data collection. The figure is based on field survey results, review of literature (Diepenbrock et al., 2012; KBTL, 2009; LWK-NRW, 2008; Meier, 2001; Munzert, 2006) and local newspaper articles regarding harvesting dates.

1:25,000 and a model accuracy of ± 3 m (AdV, 2006). For the remote sensing-based crop mapping, the spatial information of the transportation network was utilized to register all remote sensing images to the same spatial reference in ArcGIS (transformation method: adjust) (Waldhoff and Bareth, 2009). Additionally, the road network was used to improve the delineation of agricultural areas in the further analysis.

3.2. Physical blocks

The physical blocks (PB), in German 'Feldblöcke', contain the entire agricultural area of NRW on an annual basis as polygon features and are provided by the Chamber of Agriculture of North Rhine-Westphalia. In NRW, the physical blocks are the spatial entity of the German Land Parcel Identification System (LPIS) and the basis for agricultural subsidies in the framework of the European Common Agricultural Policy (CAP) (BMELV, 2004; EU, 2009; LWK NRW, 2005). They are, therefore, considered as the most comprehensive, accurate and up-to-date dataset available to delineate arable land in the study area. Individual physical blocks consist of coherent land parcels of the same principal agricultural land use type (i.e. mainly arable land, permanent crops and grassland) and are bordered by a persistent enclosing like roads, rivers or forest (LWK NRW, 2011). Although no single agricultural parcels with only one crop type are differentiated, the physical blocks were used to create an arable land mask for the remote sensing classifications. Thus, the confusion of crops and pasture is not possible in the image classifications.

3.3. Remote sensing data and pre-processing

To obtain a sufficient spatial and temporal coverage of the study area on an annual basis, and at low data costs, the incorporated multispectral remote sensing systems comprised ASTER, Landsat-5-8, IRS-P6, SPOT 6/7 and RapidEye. Table 2 summarizes the main characteristics of the systems.

For the analysis, all datasets were registered to a reference grid, based on the rasterization of the ATKIS transportation network with 15 m spatial resolution. On the one hand, the 15 m pixel size was the desired spatial resolution for the regional agro-ecosystem modeling approach of the research project, where our study is located in. Additionally, this resolution allows the differentiation of single parcels with regard to the size spectrum of crop parcels in the study area and to maintain computation efficiency. On the other hand, the spatial resolution of the ASTER data was also a good compromise in terms of data resampling in-between the spatial resolutions of the predominantly used imagery from RapidEye (5 m), ASTER (15 m), and Landsat (30 m). For the spatial resampling of the RapidEye data, all input pixel values that contributed to the coarser output pixel were averaged (pixel aggregate). The spatial resampling of the satellite imagery with a

Table 1
Crop phenology-related acquisition windows for multispectral remote sensing data collection.

Acquisition window	Approximate time period	Main classification aims
1	End of April–end of May (ca. 15.04–25.05)	• Winter cereals, rapeseed • Bare ground (summer crops) • Summer cereals (esp. spring barley) • Early potatoes
2	Start of June–mid-June (ca. 01.06–15.06)	• Differentiation of winter wheat and winter barley • Summer cereals • Potatoes
3	Mid-July–start of August (ca. 15.07–07.08)	• Harvest of winter barley (esp. in the north) • Potentially differentiation of potato, sugar beet
4	2.Half of August (ca. 15.08–31.08)	• Harvest of rapeseed, winter wheat and winter rye • Harvest in southern part (esp. spring barley) • Differentiation of maize, sugar beet and potato
5	1.Half of September (ca. 01.09–15.09)	• Differentiation of maize, sugar beets and potato

Table 2
Incorporated multispectral remote sensing systems.

System (sensor)	Multispectral bands (no.)	Spatial resolution (m)	Swath width (km)	Revisit time (days)
ASTER (VNIR)	3	15	60	16
RapidEye	5	5	77	1 (theoretically)
IRS-P6 (LISS III)	4	23.5	141	14
Spot 6/7	4	6	60	< 3 (viewing angle < 45°)
Landsat-5, 7, (8)	7, (8) [@ 30 m]	30	185	14.5

coarser pixel size than target spatial resolution, were usually resampled using nearest neighbor. Only in cases where the registration of the imagery to the transportation network caused strong distortions, occasionally bilinear or cubic convolution was used instead. These resampling procedures and the usage of imagery with a coarser spatial resolution than the target pixel size were considered as valid, since only arable land areas, as indicated by the physical block data, was needed. Consequently, all other areas were discarded for the further analysis. Finally, since only categorical information was desired, no atmospheric correction was applied for the remote sensing analyses (Song et al., 2001).

4. Methods

The annual multitemporal crop type mapping is separated into a remote sensing part (Section 4.1) and a GIS part (Section 4.2) following the Multi-Data Approach (MDA) proposed by Bareth (2008). For both parts, the crop type-specific phenology was taken into account. In Section 4.3 the MDA methodology for the crop sequence data generation and the succeeding crop rotation mapping is illustrated.

Concerning the terms we have used to describe the succession of the major crops on a parcel from year to year, we generally follow the definitions given by Leteinturier et al. (2006). Correspondingly, 'crop sequence' indicates (just) the succession of the crop types in a defined time span. In contrast, the term 'crop rotation' refers to certain multiannual crop pattern, which is repeated multiple times, is connected to a cropping system and is usually intended to have positive effects on the agro-environment or the crop yield.

4.1. Annual remote sensing crop type classification (RS-part)

In the remote sensing-part for the annual crop mapping every image was classified individually using the supervised pixel-based classification methods Maximum Likelihood (MLC) (Richards, 2012) or alternatively Support Vector Machines (SVM), as implemented in the Environment for Visualizing Images (ENVI), versions 4.4–5.3. The parametric MLC has been the standard classification algorithm in remote sensing for over four decades. With MLC, pixels are assigned to the class with the highest probability using variance and covariance matrices of the training data, which is as a whole assumed to be normally distributed (Jensen, 2016). MLC enables comparatively fast and robust classification results, if enough training data is available and data dimensionality is not too high (Richards, 2012), which is the case in our study. The non-parametric SVM builds on machine learning theory (Vapnik, 1995). SVM have been very popular in remote sensing in the past decade. SVM make no assumptions on the data and are known to generalize well even with only a small amount of trainings samples (Mountrakis et al., 2011). In contrast to MLC, SVM incorporate training samples lying rather at the margins of the training class distributions to discriminate classes, while discarding samples from the center (Foody and Mathur, 2004).

To allow satisfying classification results, extensive ground reference data surveys were conducted annually. The pink areas in Fig. 1 indicate the parcels, which were visited in total for crop type reference data collection in the field in the eight years (note: not all parcels could be visited in each year). The different clusters represent regions with different crop type composition and environmental conditions. In the field survey for 2015 about 770 parcels (3226 ha in total) were mapped (light green areas in Fig. 1). The number of mapped parcels per crop type ranged between 38 for maize and 166 parcels for winter wheat. In many cases, parcels were visited multiple times during a growing season to estimate crop management like the beginning of harvest. Additionally, it was tried to revisit many parcels from year to year to obtain reference crop sequences from the field survey data. From this data basis, different sample sets were selected for training and validation for each classification (usually at least 50% were used for validation). Training sample selection was applied following Foody and Mathur (2006) incorporating also mixed boundary pixels for an improved class differentiation, especially regarding SVM. For comparison, the same training sample sets were used for both classifiers. Training sample selection was verified using Jeffries-Matusita Distance and Transformed Divergence (Richards, 2012). The number of pixels used as training samples varied between different acquisition dates, sensor types, and coverage areas of the imagery. For the image classifications of 2015 the number of training pixels ranged between ca. 100 and more than 5000 per crop class. Normally these pixels were taken from at least 10 different parcels, which were distributed over the field survey area (cf. Fig. 1). All MLC and SVM (selected kernel type: Radial Basis Function) classifications were performed with the default settings in ENVI (ExelisVis, 2015a, 2015b). Afterwards, the classification results were slightly smoothed using Include Classes for ENVI (Gagliano, 2007) by assigning groups with a maximum of four pixels to neighboring classes.

Classification performance was validated per crop class prior to the filtering using standard error matrices incorporating mainly the User's Accuracy (UA) and the Producer's Accuracy (PA). Additionally, the Overall Accuracy (OA) and Kappa coefficient (K) were taken into account (Congalton and Green, 2009). The error matrices calculation incorporated only pixels, which were not used for the training. The number of validation pixels per crop class usually exceeded the number of training pixels considerably and was taken from even more parcels per crop type. The number of pixels used for the validation of the classification results of 2015 and for the final annual crop maps can be found in Supplements B and C, respectively.

The general crop classification procedure for every image generally started with MLC, because of the significantly lesser computation time. However, if no satisfying result was achieved, SVM was applied alternatively. In such cases, the classification result with the higher PA/UA value combination for the mainly targeted crop classes was chosen for the further analysis. Since the remote sensing results were only the first step for the crop type differentiation, the maximization of the overall classification performance was not essentially needed at this stage. Nevertheless, the primary goal of the presented approach was the direct classification of crops with a high accuracy (ca. > 85 %).

In connection with the concept of crop phenology/management and the related crop type appearance in multispectral remote sensing imagery (Sections 2.2 and 2.3), the classification of (only) specific crop classes was targeted for each time step (cf. Fig. 3). In Fig. 3, the approximate time periods are labeled with the (crop) classes, which are most likely classified with a high accuracy (PA & UA). In accordance

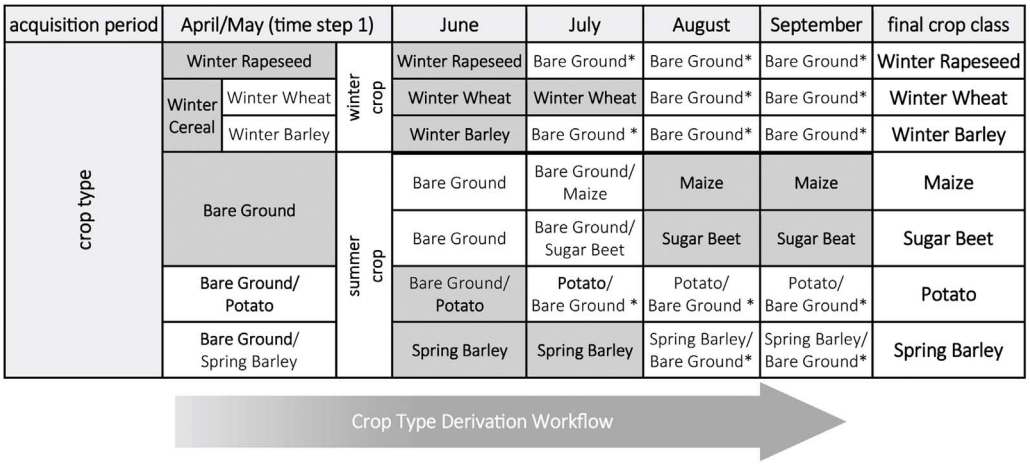

Fig. 3. Knowledge-base and workflow diagram for the formulation of production rules and the derivation of the final annual crop classification maps. Crop type terms in bold (also gray background) indicate optimal time step domains for the identification of the specific crop type. Regular case terms or dual labeling indicates uncertain cases. Bare Ground * = harvested.

with the acquisition window (AW) definition (Fig. 2), again some crop classes are assigned to multiple time periods (most optimal cases in bold characters). In contrast, combinations of two classes indicate possible uncertainties in the differentiation of the specific crops. Note, the time periods in Fig. 3 are less definite, since the actual remote sensing data basis often not optimally matched with the designated acquisition window (Fig. 2). The annual multitemporal image classifications were applied in the order of acquisition of the time steps, starting with the first. The class composition for each subsequent time step was adapted depending on the previous results.

4.2. Annual Multi-Data Approach crop type determination (GIS-part)

For the post-classification generation of the final annual crop maps in the GIS-part of the Multi-Data Approach, all time step classifications and ancillary data layers were stacked together (in the following referred to as MDA-Grid) using the ESRI grid format (ESRI, 2012a). On ESRI grids containing only categorical information, knowledge-based production rules can be applied by using Structured Query Language (SQL) and field calculation functions in ArcGIS (ESRI, 2012b; Heywood et al., 2011; Kappas, 2011). In this way, information of the individual time step classifications was directly extracted or connected with other information to derive the final crop classification result, like:

Select From MDA-Grid WHERE:

physical blocks = arable land
AND time step 1 = winter crop
AND time step 2 = winter wheat

In this example, selected pixels are labeled with the crop class winter wheat. For the formulation of such crop type specific production rules, Fig. 3 also portrays the underlying knowledge-base and the general workflow. As can be seen from the example, all production rules were additionally restricted to arable land only, using the physical block data as stratification layer (cf. Section 3.2). In this way, it was impossible to assign a crop class outside of arable land, in case no arable land masking was applied beforehand. Besides this, the generation of the final annual crop maps by means of applying production rules was targeted using three basic strategies:

(i) extraction of mutually exclusive summer crop and winter crop areas,
(ii) direct transfer of the best crop specific classification results, leading to a successive reduction of areas to be assigned with a crop class,
(iii) derivation of the crop class membership for pixels, where no direct class allocation was possible, by connecting the pixel-specific sequences of the time step classification results with the projected course of class allocation per crop type (cf. Fig. 3).

In accordance with the general analysis workflow, the generation of the final crop maps started with the utilization of the classification result of acquisition window 1/May (usually equals time step 1) to disaggregate arable land by integrating crop type classification results. As can be seen from Figs. 2 and 3, at acquisition window 1, all winter crops are present in a closed canopy situation on arable land. In contrast, areas designated or prepared for the summer crops maize, sugar beet and potatoes are already cleared from catch crops (where applicable) and exhibit bare soil. Summer crop parcels containing spring barley or early potatoes occasionally already show (rather weak) vegetation signals in acquisition window 1, if weather conditions led to comparatively premature vegetation development in one year. Nevertheless, the differentiation of bare soil, soil/vegetation mixtures and closed-canopy vegetation on arable land at this time period, leads to a fundamental separation of summer crop areas and winter crop areas for most regions. Consequently, based on the resulting crop group mask layer, summer crop areas and winter crop areas are treated separately in the following analysis (strategy i) to reduce misclassification.

Concerning direct crop classification, time step 1 is also most favorable to separate winter rapeseed from winter cereals. Hence, introducing strategy (ii), high accuracy classification results (e.g.) of winter rapeseed in time step 1 were directly transferred to the final classification result. However, for the differentiation of cereal types, remote sensing data of acquisition window 2 (usually time step 2) is more appropriate.

By working chronologically through the workflow chart (Fig. 3), the targeted crop class classification results were successively extracted from the appropriate time steps. For crop types that were accurately classified in multiple time steps, the result with the highest UA/PA was predominantly transferred to the final crop classification map. Occasionally, multiple time step classification results were used to optimize the crop class coverage, if high accuracies were achieved in each case. Pixels, for which the ultimate crop class was determined with a high accuracy, were concurrently masked out for the further analysis. In analogy to approaches like Van Niel and McVicar (2004) this sequential procedure resulted in an incremental reduction of pixels that had to be labeled with a final crop class.

However, depending on the available remote sensing data basis, for some areas direct crop type identification was not always possible. For the handling of such cases, Fig. 3 again represented the knowledge-base for the production rule creation. For this purpose, the course of class

allocation of these areas or pixels in the consecutive time step classification results was compared with the different model sequences of class allocation in Fig. 3 (strategy iii). For example, within the five time steps, the typical course of class allocation to result in the final crop class winter wheat would be:

1. winter cereal 2. winter wheat 3. winter wheat 4. bare ground

5. bare ground=winter wheat

To improve the crop type differentiation, the information in Fig. 3 could be used in the following way. Winter barley, for instance, is generally harvested prior to winter wheat in the study area. Thus, if a significant number of pixels was classified as bare ground (Bare Ground*) in a time step of late July and on a winter crop area, and the same pixels were assigned to a winter cereal class in a preceding time step, this combination was utilized to refine the differentiation of winter wheat and winter barley (cf. Fig. 3).

As stated in Section 2, winter rye is also cultivated in the eastern part of the study area. However, due to the high similarity to winter wheat, and although the phenology was considered, it was not possible to satisfactory differentiate both crop types in this study. Therefore, winter rye had to be equated with winter wheat.

4.3. Crop sequence and crop rotation mapping methodology

In accordance with the annual crop mapping, the study area-wide crop sequence data generation was based on the spatial integration of the multiple annual crop mapping results using GIS overlay analysis methodology. For the current study, crop maps of the eight consecutive years 2008–2015 were incorporated. Due to performance advantages, all crop sequence and crop rotation analysis tasks were conducted in the vector data model in ArcGIS. Accordingly, all annual crop maps were transferred into vector data. The geometrical structure of the raster cells was maintained for the conversion. Afterwards, additional data preparation tasks were conducted. Fig. 4 illustrates the workflow of the crop sequence data generation.

Owing to the pixel-based nature of the annual results, isolated pixels or small pixel groups of rather questionable class allocation were present in the annual crop maps. This was especially true for parcel or land use borders. For the reduction of such cases, a slight generalization (I) of the individual crop maps was performed. By using the Eliminate-Tool in ArcGIS (ESRI, 2016b) small isolated areas (size ≤10 pixels) were assigned to neighboring polygons with the longest shared border. This procedure was repeated three times to compensate for small areas that were set free through dissolving multipart polygons in intermediate steps. Afterwards, all annual crop maps were spatially integrated to a single data layer using the Union-Tool in ArcGIS (ESRI, 2016c). Through this step, the multiannual crop type information was already assigned to discrete areas. However, multitemporal image classification results of the same area, were sometimes characterized by location shifts of class borders of one or two pixels between the individual classifications, although the position of the underlying border had not changed in reality. Through the spatial integration (union) of the multiple classification results, each of these pseudo class border shifts propagated to the final crop sequence dataset. On the one hand, this led to an increased spatial fragmentation of such class border regions into several smaller patches (comparable to sliver polygons) in the resulting single layer dataset. On the other hand, also the total number of areas with individual crop sequences increased. To reduce the number of such overlay artifact areas, the Eliminate-Tool was again iteratively applied to remove areas ≤3 pixels (generalization II). In the last data processing step, the crop sequence information was generated by the combination of the year-specific crop class information to a unique crop sequence string for every polygon, using the Field Calculation-Tool in ArcGIS (ESRI, 2016a). On this data basis, knowledge-based production were applied to identify crop rotations. This was done by creating standard query language-commands to examine the crop sequence dataset for certain crop succession strings or to investigate the frequency of occurrence of typical crop rotations.

5. Results

In Section 5.1 the preconditions for the annual crop type mapping related to the remote sensing data basis, the execution of the analysis and the achieved results are exemplarily described for the year 2015. Information about the remote sensing data incorporated for the other years as well as the full error matrices can be found in supplements A and C, respectively. In Section 5.2, the results for the integration of the annual crop maps into one crop sequence dataset and the analysis of this data concerning the identified crop sequences and crop rotations are presented. In Section 5.3 the remote sensing data-based crop sequence and crop rotation mapping results are compared with our field survey data.

5.1. Annual crop mapping result for 2015

In Fig. 5 the spatial coverage of the input imagery for the crop mapping of 2015 is presented. As can be seen from Fig. 5, full or cloud free spatial coverage of the study area was not available for any acquisition date. Because of this fragmentation, the analysis had to be separated into several parts. Additionally, scenes acquired outside of the defined acquisition windows had to be incorporated to approach sufficient coverage. Indeed, this was the case in all of the years (2008–2015), due to frequent cloud cover throughout the year.

For the description of the crop mapping of 2015, the explanations are focused to the area of Subset I (marked as a red box in Figs. 1 and 5). The classification results for each scene are displayed in Fig. 6. The scenes of May 15th and July 11th were not used for this area. All scenes

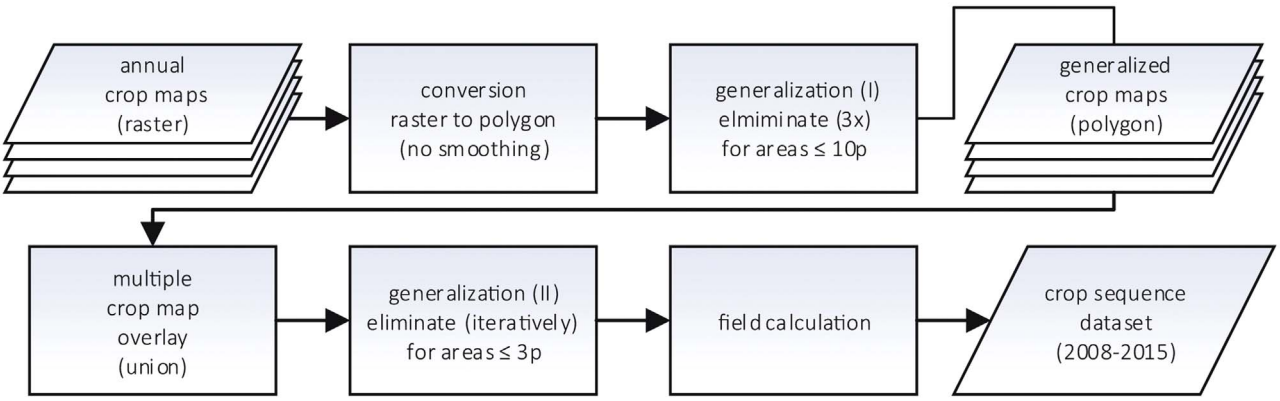

Fig. 4. Workflow of the crop sequence dataset generation (p = pixel area).

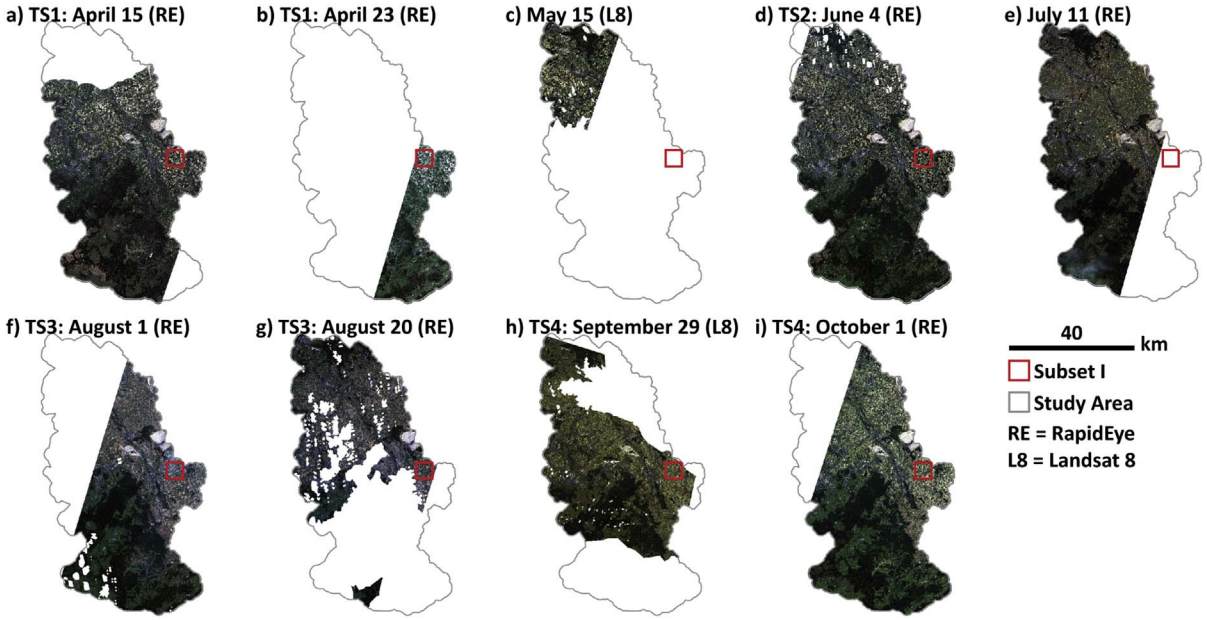

Fig. 5. Remote sensing scenes available for the crop mapping 2015, resulting in four time steps for Subset I. Scenes are clipped to the study area extent.

were classified with MLC, using mainly the designated crop classes according to Fig. 3. The corresponding UA und PA values for the time step classifications and the final crop map are listed in Table 3. The full error matrices of the time step classifications of 2015 can be found in supplement B. Basic information about the training data used for the classifications is provided in Section 4.1.

Beginning with time step 1, winter crop and summer crop areas were fundamentally differentiated based upon the classifications of April 15th and April 23rd (building time step 1). At this time, a closed canopy was already developed by the main winter crops (winter wheat, winter barley and winter rapeseed), while on summer crop parcels the main summer crops maize, potatoes, sugar beet as well as spring barley were just sown, thus appearing as bare ground. In addition, winter rapeseed was separated from winter cereals in this time step. As final step for time step 1, mainly the classification results from April 23rd were transferred for Subset 1, because of the more proceeded plant development. However, for nodata areas in the scene of April 23rd, classification results from the scene of April 15th were used. Furthermore, results for winter barley were also taken from the classification of April 15th.

From time step 2 (June 04th) a refined segregation of winter wheat and winter barley parcels was extracted. In addition, root crops (potatoes, sugar beets) and spring barley were already detectable, which led to a first disaggregation of summer crop areas. Time step 3 was composed of the classifications of 1st of August and August 20th. However, for Subset I the former classification was not needed. At

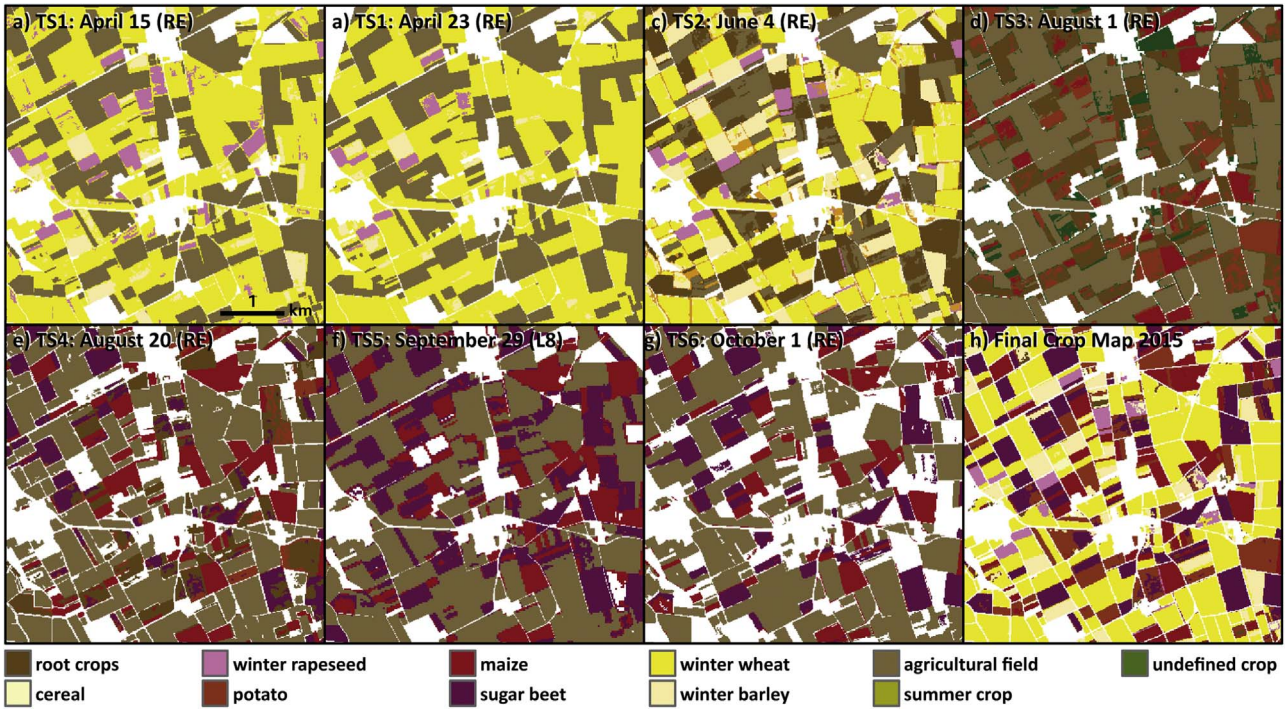

Fig. 6. Time step classification results and the final crop map of 2015 for Subset I (cf. Fig. 1).

Table 3
Producer's accuracy (PA), user's accuracy (UA), overall accuracy (OA) and kappa (K) for the time step classifications and for the final crop map 2015 (the full error matrices are provided in supplement B).

Crop class	April 15		April 23		June 4		August 1		August 20		September 29		October 1		2015	
	PA	UA	PA	UA	PA	UA	PA	UA	PA	UA	PA	UA	PA	UA	PA	UA
Root crops					99.32	96.11	46.64	53.83								
Bare ground	97.44	99.64	98.1	100.00			98.86	85.55	99.97	93.92	85.23	98.34	98.33	98.14		
Winter rapeseed	91.86	82.02	85.90	100.00	98.11	99.62									98.36	99.98
Winter wheat	91.27	75.70	96.67	81.13	78.54	99.62									98.62	97.43
Winter barley	27.08	74.43	1.13	4.33	98.73	59.47									95.89	92.84
Sugar beet									70.11	97.98	89.51	75.17	88.65	95.93	96.20	98.36
Potato							34.14	30.77	68.21	54.28					96.74	95.14
Maize							69.42	78.33	99.80	95.96	97.77	61.49	99.94	87.77	100.00	98.59
Spring barley					90.41	94.68									95.08	99.47
Undefined crop					30.51	65.28										
OA	87.32		91.86		89.62		73.51		88.63		87.75		96.88		97.43	
K	0.80		0.87		0.87		0.57		0.81		0.75		0.92		0.97	

August 20th all winter crops were harvested or not spectrally detectable as green vegetation (classified as bare ground). Thus, time step 3 contributed to the disaggregation of maize, sugar beets and potatoes. However, spectral similarities still hampered the clear differentiation, as noticeable from the corresponding PA and UA values (Table 3). Consequently, classifications of September 29th and 1st of October (time step 4) were additionally included. Here, mainly data of the 1st of October were used, while September 29th (Landsat-8) was only incorporated to fill data gaps. At this stage, potatoes were already harvested, but sugar beets were still on the fields. Thus, it was possible to disaggregate both crops to a certain level, by ruling out vegetated from non-vegetated fields in comparison with preceding dates. Finally, classification results of both dates were used to ascertain the location of maize parcels in the final crop map (Fig. 6h).

5.2. Crop sequence data and crop rotation mapping result (2008–2015)

The annual crop mapping results for the years 2008–2015 are the foundation for the generation of the crop sequence dataset to perform the crop rotation mapping. For comparison, Fig. 7a–h depicts the annual crop mapping results for Subset I (cf. Fig. 1), before the additional generalization procedures where performed.

Additionally, for the estimation of the quality of the information provided by the crop sequence dataset, Table 4 summarizes the corresponding crop type specific PA and UA values for all years, except for 2012, where no validation data was available. In general, comparatively stable crop type-specific PA and UA were achieved for all years. Nevertheless, especially winter barley and potato are characterized by degraded accuracies in some years. As can be seen from the full error matrices (cf. supplement C), this is usually attributed to the incomplete spectral differentiation of winter wheat/winter barley and sugar beet/potato. However, both winter wheat and sugar beet surpass their counterparts significantly in cultivation area in the study region (IT.NRW, 2012).

After the integration of the eight annual crop maps to a crop sequence layer, 154,259 individual areas with crop sequences are differentiated in the final dataset (94,393 ha in total). On these areas 15,908 individual eight-year crop sequences were identified (72,153 ha in total), which have a total area of larger than 1 ha and contain a crop type in each year. All crop sequences with a smaller area were regarded

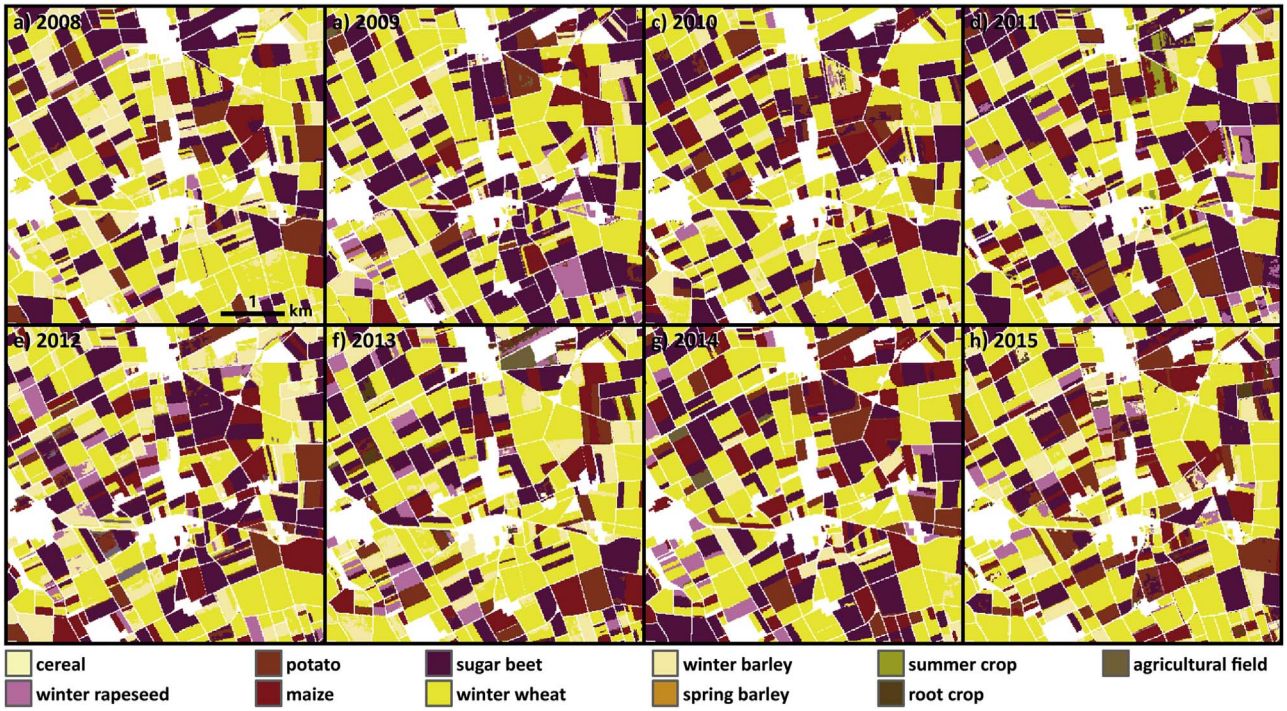

Fig. 7. Subsets of the annual crop mapping results for 2008–2015 for Subset I (cf. Fig. 1).

Table 4
Crop type specific producer's accuracy (PA) and user's accuracy (UA) for the land use maps 2008–2011 and 2013–2015 (Lussem and Waldhoff, 2013a,b; Lussem and Waldhoff, 2014, 2015; Waldhoff, 2012a,b,c; Waldhoff and Lussem, 2016).

Crop class	2008		2009		2010		2011		2013		2014		2015	
	PA	UA	PA	UA	PA	UA	PA	UA	PA	UA	PA	UA	PA	UA
Winter rapeseed	93.93	100.00	99.80	99.39	99.80	99.93	92.54	84.66	98.99	99.55	99.02	95.68	98.36	99.98
Winter wheat	92.21	89.40	97.73	84.71	95.14	90.94	97.01	92.12	93.47	69.68	95.01	89.93	98.62	97.43
Winter barley	86.59	87.14	73.56	92.55	80.88	88.59	61.00	88.84	45.51	81.07	74.59	86.84	95.89	92.84
Sugar beet	96.17	94.58	100.00	81.95	97.97	88.28	95.63	75.32	91.55	96.09	94.89	95.41	96.20	98.36
Potato	88.50	91.82	31.12	100.00	75.19	97.87	34.43	91.76	71.19	69.55	95.50	94.33	96.74	95.14
Maize	94.72	97.20	97.97	100.00	97.48	95.25	92.38	84.64	93.19	78.42	92.05	86.19	100.00	98.59
Spring barley	94.42	96.57	93.01	97.51	92.17	96.62	93.58	79.77	79.34	97.57	59.77	94.95	95.08	99.47

Table 5
The 10 major crop sequences of the study area (in terms of total area), always starting from 2008 and ending 2015. WW = winter wheat, WB = winter barley, WR = winter rapeseed, SB = sugar beet, P = potato, M = maize, SPB = spring barley.

Rank	Crop sequence	Total area (ha)	% of total area
#1	SB-WW-WW-SB-WW-WW-SB-WW	742	0.79
#2	WW-SB-WW-WW-SB-WW-WW-SB	490	0.52
#3	SB-WW-WB-SB-WW-WB-SB-WW	473	0.50
#4	SB-WW-WW-SB-WW-WB-SB-WW	384	0.41
#5	WW-WB-SB-WW-WW-SB-WW-WB	383	0.41
#6	SB-WW-SB-WW-SB-WW-SB-WW	351	0.37
#7	WW-WW-SB-WW-WW-SB-WW-WW	348	0.37
#8	WW-WW-SB-WW-WW-SB-WW-WB	325	0.34
#9	SB-WW-WB-SB-WW-WW-SB-WW	294	0.31
#10	SB-WW-P-WW-SB-WW-P-WW	283	0.30

as negligible for the analysis.

Out of the whole crop sequence dataset, Table 5 lists the 10 major crop sequences (in terms of total area) that include a crop class in all of the eight years. All other individual crop sequences account for less than 0.3% of the study area. In the table, the underlining marks the identified crop succession links, which already are identified crop rotations, or built the foundation of crop rotations (e.g. root crop – cereal or root crop – cereal – cereal) (Munzert, 2006). As can be seen, even the most frequent eight-year crop sequence comprises less than one percent of the total study area. All of the crop sequences are dominated by sugar beet (SB) and winter wheat (WW), with winter barley (WB) being third in terms of contribution. In this regard, crop sequences in which winter wheat follows sugar beet or vice versa at least once, comprise 68,292 ha and 72% of the study area. Additionally, seven crop sequences in Table 5 include the direct repetition winter wheat ('WW–WW') once or even multiple times, which is generally regarded as rather contradictory to good farming practice. Taking all crop sequences with WW–WW-links into account, 41% of the study area is occupied by such crop sequences. By complementing the crop sequences with regard to the identified crop succession patterns, repetitions of actual crop rotations can be identified. Accordingly, the crop sequences #1, #2 and #7 in Table 5 are most likely repetitions of the 3-year crop rotation 'SB–WW–WW (sugar beet–winter wheat–winter wheat)', only captured at different temporal stages. The combination of these crop sequences, which (most likely) only contain continuous repetitions of this crop rotation results in the most dominant crop rotation with a proportion of 1.67% of the study area in this regard. In the same manner, for instance, crop sequence #3 can be regarded as a repetition of the common "Rhenish Crop Rotation" (SB–WW–WB, sugar beet–winter wheat–winter barley). Not until rank #10, a crop sequence includes an additional crop type (in this case potato).

However, when querying typical crop rotations of durations from 2 to 5 years, much larger areas are covered. Table 6 list a selection of crop rotations identified within the crop sequence dataset. For example, crop sequences that include the crop rotation 'SB–WW–WW' at least once

Table 6
Selected crop rotations identified in the final crop sequence dataset 2008–2015 (values are rounded) at least once in an eight-year sequence. WW = winter wheat, WB = winter barley, WR = winter rapeseed, SB = sugar beet, P = potato, M = maize, SPB = spring barley.

	Crop rotation	Total area (ha)	% of total area
2-Year	SB-WW	61,855	66
	SB-SB	11,797	13
	WR-WW	19,775	21
3-Year	SB-WW-WW	21,840	23
	WR-WW-WB	4415	5
	WR-WW-WW	5060	5
	SB-WW-WB	13,290	14
	SB-WW-P	8890	10
	SB-WW-SB	17,550	19
	M-WW-SB	6870	7
	M-WW-M	5220	6
4-year	SB-WW-P-WW	5240	6
	SB-WW-SB-WW	10,870	12
	SB-WW-M-WW	4003	4
5-year	SB-WW-WW-SB-WW	8990	10
	SB-WW-WB-SB-WW	5090	6
	SB-WW-SB-WW-SB	3580	4
	SB-WW-P-WW-SB	2340	3
	WW-M-WW-M-WW	1280	2

account for 23% of the study area, while the "Rhenish Crop Rotation" (see above) still is conducted on 14% of the study area.

To illustrate the crop sequence and crop rotation mapping, Fig. 8 depicts the area of Subset II (cf. Fig. 1). In Fig. 8 every tint of gray represents a unique crop sequence. Accordingly, on areas with the same gray tone, identical successions of the main crops were determined. Subset II, for example, comprises 3875 individual areas (4010 ha in total), on which 2607 different crop sequences were detected. Within Subset II the crop sequence 'SB–WW–WW–SB–WW–WW–SB–WW' ('h' in the legend of Fig. 8) has the highest count with 16 occurrences (33 ha in total), whereas the crop sequence 'P–WW–SB–WW–P–WW–SB–WW' ('b' in the legend of Fig. 8) has the highest total area (53 ha, recorded three times). The colored areas (other than gray) mark the parcels on which the 50 major crop sequences within Subset II occur (in terms of total area). As can be seen from the legend of Fig. 8, again crop sequences with a very similar structure and only two or three crop types, can be differentiated from more heterogeneous crop sequences with up to five different crop types. In Addition to the coloring, some areas in Fig. 8 are highlighted by a colored delineation, resulting in 10 individual groups. In these groups, crop sequences are combined, which were regarded as the repetitions of the same crop rotation or connections of multiple crop rotations, only captured in a different temporal stage. Consequently, for example, the yellow colored parcels contain different temporal stages of the study area-wide most dominant crop rotation 'SB–WW–WW'. Although this crop rotation only occurred on 34 parcels, it is the most frequent crop rotation in Subset II (with a total

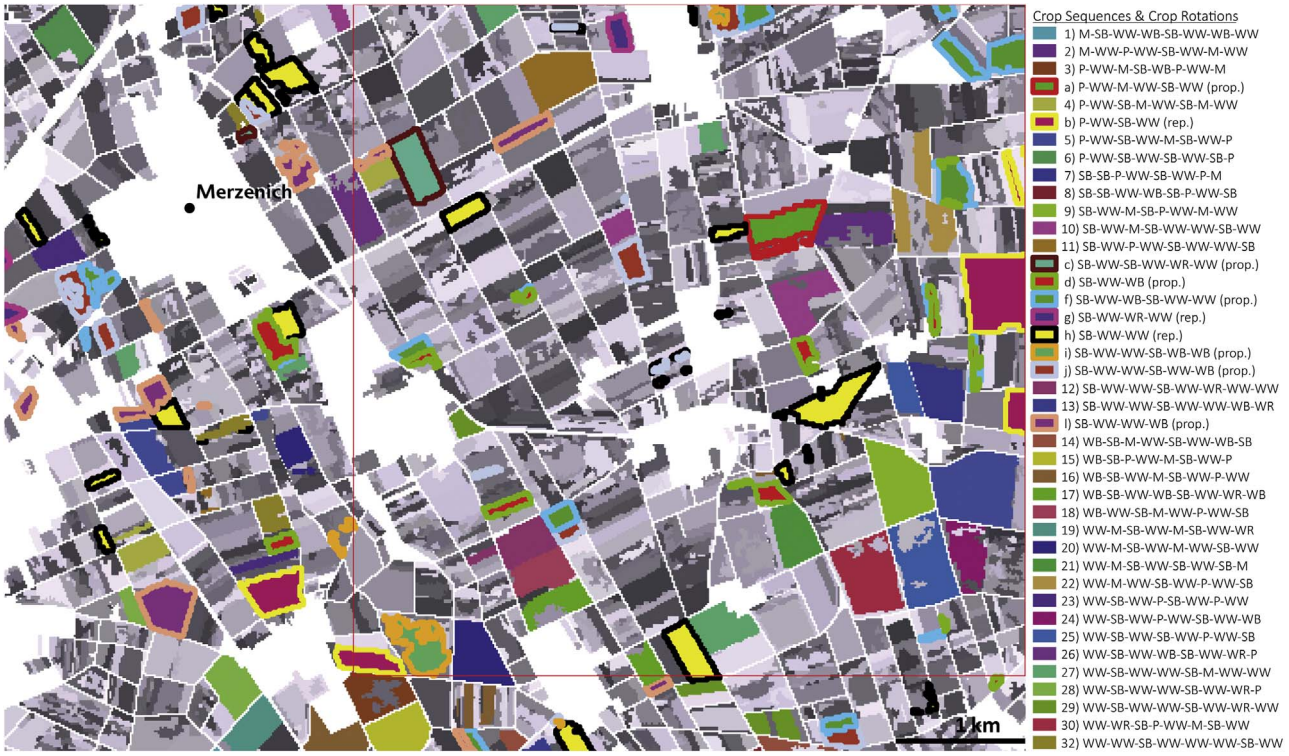

Fig. 8. Map of selected crop sequences and crop rotations (2008–2015) out of the 50 most frequent crop sequences in terms of acreage in Subset II (cf. Fig. 1), as an extension of Subset I (red box). Colored areas highlight the most frequent crop sequences (numbers in the legend). Additionally, areas on which typical crop rotations occur (but possibly at different stages) are grouped by a colored delineation (letters in the legend). WW = winter wheat, WB = winter barley, WR = winter rapeseed, SB = sugar beet, P = potato, M = maize, SPB = spring barley. (For interpretation of the references to color in this figure legend, the reader is referred to the web version of this article).

Table 7
Field survey crop sequences (2008–2015) for selected parcels, which were identically recorded in the crop rotation map. Crop types in italic mark the year 2012, where no field data was available (further explanations in the text). The underlining marks common crop type links and crop rotations.

Number	Crop sequence
1	SB-WW-WW-SB-*P*-WW-SB-WW
2	SB-WW-WW-SB-*WW*-WW-SB-WW
3	SB-WW-WB-SB-*WW*-WW-SB-WW
4	SB-WW-SB-WW-*WR*-WW-SB-WW
5	SB-WW-SB-WW-*WR*-WW-SB-P
6	P-WW-SB-WW-*WW*-SB-M-WW
7	P-WW-SB-WW-*WR*-WB-P-M
8	P-WW-SB-P-*WW*-WR-P-M
9	SB-WW-WW-SB-*WB*-SB-M-WW
10	SB-WW-WB-SB-*WW*-M-WW-SB

area of 78 ha). Furthermore, in analogy to the whole study area, again 15 crop sequences of the 50 major crop sequences contain the link WW–WW at least once. Finally, considering all crop sequences within Subset II, such crop rotations, which include the direct repetition of winter wheat, occur on 44% of this area.

5.3. Comparison of the remote sensing-based mapping results with field survey data

To evaluate the accuracy of the crop sequence dataset and the crop rotation mapping results, two separate analyses were conducted by incorporating the crop sequence information derived from our field survey data (2008–2011 and 2013–2015).

The first analysis was related to the large amount of crop sequences with direct repetitions of winter wheat (2× or more) identified from the remote sensing-based dataset. As stated in Sections 4.2 and 5.2, it was not possible to differentiate winter rye from winter wheat at all, and winter wheat was sometimes confused with winter barley. Thus, these confusions could have significantly influenced the number of cases of the direction repetitions of winter wheat. To estimate this, the field survey data for the years 2008–2011 was examined. From this dataset, all parcels containing one of the major crop types in each year were selected. This dataset also included 31 parcels with winter rye, which was always mapped in the field surveys. From the 132 resulting parcels, 28 crop sequences included the direct repetition of winter wheat ('WW–WW') at least once (approx. 21%). Furthermore, from these 28 crop sequences, three crop sequences included triple repetitions ('WW–WW–WW') and even winter wheat in all of the four years was mapped once.

In the second field survey data analysis, the wide spectrum of individual crop sequences and crop rotations was investigated. Therefore, the field survey results for the years 2013–2015 were added to the 2008–2011 data. This resulted in 60 parcels with a mapped major crop type for the time span (2008–2015), except for 2012 where no ground reference data was available. For the sake of completeness, the 2012 crop types were therefore taken from the remote sensing-based crop map. Table 7 lists a selection of the field survey crop sequences. None of the field survey crop sequences was mapped twice. This was the main reason, why we did not find an appropriate way until now, to conduct an error matrix-like accuracy assessment. Accordingly, we compared the field survey results with the crop sequence dataset using the center point of the field survey parcels. On this basis, the recorded crop sequences were identical on 26 parcels (ca. 42%) in the two datasets. On 20 other parcels (ca. 33%) only a single confusion within root crops (maize, potato, sugar beet) or between cereals (winter wheat, winter barley, spring barley) occurred. The group of the remaining 14 crop sequences (23%) was composed of crop sequences with single confusions between root crops and winter cereals (e.g. between maize and winter wheat) or up to three confusions.

6. Discussion

6.1. Crop rotation mapping results

Our primary goal was the mapping of practiced crop rotations in our study region from remote sensing-derived crop sequences data. Based on our results, the question, if the actually occurring spatio-temporal land use patterns on arable land are realistically represented by the usage of prototype crop rotations in regional scale agro-ecosystem modeling or not, can be clearly answered with no. Despite certain methodological and data quality aspects (discussed in Section 6.2), the results of this study show that our Multi-Data Approach is capable of providing detailed information on the spatial distribution of crop sequences and crop rotations for a regional scale (3400 km^2 in 1:25,000). The crop sequences and crop rotations that we found in our study region, are most of the time completely different from crop rotations based on expert-knowledge. As the major outcome of our investigation, the spectrum of the practiced crop rotations significantly differs from the variety and number of prototype crop rotations usually used for regional agro-ecosystem modeling. The high total number of crop sequences identified from our dataset (around 16,000!) may astonish at first (even after discarding a very large number of crop sequences with very small individual area). Nevertheless, similar findings are reported by Leteinturier et al. (2006). In view of the large amount of individual crop sequences that predominantly build upon sugar beet and winter wheat, the portions of the ten major crop sequences (cf. Table 5) on the total study area, are significantly small. This should mainly be related to the fact that with every added year to a crop sequence, fewer crop sequences will exactly match each other. However, our results show that incorporating eight or more years are absolutely necessary to identify the spectrum of the practiced crop rotations and crop rotation combinations. Otherwise it would not have been possible to recognize for example that the combination of the crop rotations 'SB–WW–WW' and 'SB–WW–WB' ('h' in the legend of Fig. 8) is comparably common (3% of the area) and widely distributed over the study area. Furthermore, eight or more years are necessary to identify all possible variations of 5-year crop rotations. With the five major 5-years crop rotations we identified (mainly containing sugar beet and winter wheat) approximately 25% of the total study area are covered (cf. Table 6). Identifying the single occurrence of the five major 3-years crop rotation of the before mentioned crops, a coverage of approx. 75% is given. Still, a huge amount of crop sequences were determined, which are composed of multiple crop types and which are lasting for more than five years.

In terms of the direct repetition of certain crop types, especially the large amount of crop sequences and crop rotations containing winter wheat in two consecutive years ('WW–WW') is remarkable. This was unexpected in this degree, since being rather in disagreement with recommended farming practices (LWK NRW, 2012). In contrast to our findings, in crop rotation modeling approaches such crop rotations are considered to a much lesser extent (cf. for example Klöcking et al., 2003; Lorenz et al., 2013; Schönhart et al., 2011). In the modeling study of Lorenz et al. (2013) the amount of the self-repetition of winter wheat was calculated with 4.2%, while in our study area crop sequences with a WW–WW-repetition cover 40,000 ha, which are 41% of the total arable land. Moreover, from the identified crop rotations it can be seen that often only one year with another crop is between two WW–WW-repetitions (cf. Table 5).

To verify our remote sensing-based results as much as possible, we used reference crop sequences we mapped in the field. The first analysis of our field survey data concerning the direct repetition of winter wheat resulted in proportion of 21% compared to 41% in the crop rotation map. However, the field survey data for this analysis comprised only four consecutive years (instead of eight for the remote sensing data-based map). Nevertheless, even the influence of misclassifications (e.g. between winter wheat and winter barley) and the fact that winter rye was not differentiable from winter wheat with our remote sensing data basis (see below), cannot disprove the general trend of the remote sensing data-based results. However, a slight overestimation of the frequency of such cases might exist in the crop sequence dataset.

The comparison analysis between the remote sensing-based crop sequences and the field survey crop sequences yielded that 75% of the remote sensing-based crop sequences were correct, or contained only a single confusion (within the summer crops or within winter crops). However, 23% contained two or more classification errors in the eight-year time span. Nevertheless, the large variety of crop sequences and crop rotations identified with the presented remote sensing approach, occurred also in our multiannual ground reference dataset. Thus, defining crop rotations solely on good farming practices for regional agro-ecosystem modeling cannot be recommended. Considering the large amount of individual crop sequences, the influence on the modeling results is significant. Therefore, the spatial distribution of crop sequences has to be retrieved to derive the actual crop rotations as an input for agro-ecosystem models like the DNDC (Giltrap et al., 2010) or the DANUBIA crop growth model (Lenz-Wiedemann et al., 2010) for the incorporated years.

6.2. Methodology and crop mapping results

With the developed methodology, an improved crop type dissemination was targeted to obtain a crop sequence database, which is suitable for regional scale crop rotation mapping. To achieve this goal, multitemporal remote sensing data, supervised classification algorithms, ancillary data for stratification of the study area, post-classification refinement and knowledge-based production rules were incorporated in a GIS environment.

For the separated analysis of crop land from other land use classes, for this study only physical blocks (PB) data, but no parcel boundary information was available. In other approaches (e.g. De Wit and Clevers, 2004; Turker and Arikan, 2005) parcel boundaries were manually added by visual interpretation of remote sensing data and manual digitizing. These individual parcels were then labeled with only one crop class by means of a majority analysis, for example. Even in case of multiple class allocations per parcel (e.g. due to misclassifications of mixed pixels at parcel borders or due to high spectral similarities of crop types, see below), such approaches lead to clear and visually appealing classification results. Although, we generally appreciate such approaches, the manual delineation of parcels was not conducted in our study. The main reason for this was that we only wanted to include already available data. Furthermore, such approaches are also not immune to misclassification, since clusters of misclassified pixels within a parcel may also lead to the misallocation of the entire parcel. As a compensation, in our Multi-Data Approach clearance of misclassification was tackled by using optimized training data, post-classification filtering and especially GIS-based analysis methods. Therefore, possible differences in classification accuracy between different classification algorithms in the range of 5% (Huang et al., 2002), usually have no impact on the final results, since the classification accuracy is further enhanced in the GIS. For this reason, slightly improving the classification results through the selection of even more sophisticated classification algorithms was not our focus in this study. In this regard, although SVM is generally regarded as the superior algorithm compared to MLC (Mountrakis et al., 2011), the SVM results were usually not significantly better. Yet, they needed considerably more computation time (i.e. minutes compared to hours). In our analysis setup, the much more influencing factor on the classification performance was the availability and the choice of training data. Hence, in our opinion, statements concerning the greater importance of the training data in comparison to the choice of the classification algorithm, e.g. Hixson et al. (1980) or Campbell and Wynne (2011), still apply.

Concerning the overall multitemporal crop classification strategy,

our Multi-Data Approach was especially designed to incorporate remote sensing data of various sensor systems. However, the desired multi-temporal coverage of our study area could seldom be met in all the years. As a result, even scenes that were acquired outside of the proposed acquisition windows (AW) had to be incorporated, where the targeted crop types were captured in rather inadequate phenological stages. Nevertheless, our approach has proven to cope with a varying and fragmented remote sensing data basis. Since considerable parts of the analysis tasks are conducted post-classification, differences in the remote sensing data source could be neglected. For the most crop classes, very satisfying results were generated annually. In most cases, this was achieved even with less than the five designated time steps. Furthermore, through the sequential masking strategy misclassifications between winter crops and summer crops were dramatically reduced. However, the differentiation of winter rye from winter wheat was not possible at all. Additionally, especially if adequate scenes out of June and late July were lacking, the differentiation performance of the crop pairs winter wheat/winter barley and sugar beet/potato was mainly affected. As a consequence, the annual crop maps also contain corresponding parcels with fragmented or mixed class allocation (cf. Fig. 7). The aggregation of such crop class couples, e.g. to classes like winter cereals or root crops, would have been another option to clear the results. However, this was refrained most of the time, since the classification accuracies still justified their preservation. In addition, with regard to the general information content of the crop maps and in view of the crop sequence and crop rotation mapping, the higher categorical detail, although including also errors, was maintained.

While the general knowledge-base for the crop differentiation (Fig. 3) always applies, the production rules had to be formulated for every subset of the study area. As a result, the workload increased with the degree of spatial fragmentation of the remote sensing data basis. However, this should apply for most studies where larger areas have to be covered. In this regard, improved conditions are expected through the additional incorporation of Sentinel-2 and Sentinel-1 data (Geudtner, 2012; Immitzer et al., 2016).

For the generation of the crop sequence dataset, the analysis focus slightly shifted from obtaining highly disaggregated information on an annual basis, toward getting a clearer picture of the existing spatio-temporal land use patterns on arable land. Therefore, serval minor generalizations tasks were performed beforehand. With this, a reasonable compromise between maintaining the original spatial structure of the annual crop maps and reducing questionable class allocations was strived. In doing so, on the one hand, losing perhaps also correct information for small areas was accepted. On the other hand, still fragmentations related to misclassification, persist in the crop sequence dataset. Nevertheless, although the dataset contains errors, it was also demonstrated from a methodological point of view that the spatial heterogeneity of the eight remote sensing-based crop type maps can be integrated into one layer from which manifold information can be obtained.

7. Conclusion and outlook

In the soil-vegetation-atmosphere system, matter fluxes related to arable land are strongly connected to the succession of different crops types (and their management) on each field from year to year. Our results, based on the investigation of eight consecutive years, clearly show that the spatio-temporal land use patterns on arable land are extremely heterogeneous in our study area. This refers to the variety of the crop types that are included in the individual crop sequences and crop rotations as well as to the immediate succession of main crop types on the parcels. Additionally, the spatial distribution of crop rotations is strongly connected to the varying cultivation areas of the different crops. This demonstrates, that it is absolutely necessary to have spatial information on the actually applied crop rotations available to conduct regional agro-ecosystem modeling. Otherwise, it is not possible to significantly reduce the uncertainties regarding the management stated by Kersebaum et al. (2007) and to assess the fluxes in agro-ecosystems properly, for a regional scale. For instance, the impact of the high number of crop rotations with the self-repetition of winter wheat should be enormously underrepresented in most cases, although the number of such cases could be slightly overestimated in our results.

Besides the provision of spatial, parcel-related crop sequence information, the spectrum of the different cropping systems applied in the study area can be identified in detail from our data. In this contribution the identification of the major crop rotations in our study area was focused. However, a comprehensive analysis to identify all occurring crop rotations was out of the scope of this study. For this task, more sophisticated production rules are needed to combine and categorize the vast amount of individual crop sequences completely. Concerning the analysis of the mapping results, the full exploitation of the crop sequence data will be the next step.

Concerning the methodological aspects, this study has proven that through the integration of remote sensing and GIS-methods with our Multi-Data Approach very complex spatio-temporal patterns, in this case for arable land, can be captured at a very high spatial resolution and for a regional scale. Through our combination of multitemporal data, ancillary information and expert-knowledge on crop phenology in a sequential analysis, crop types can be accurately differentiated even with multispectral data. However, remote sensing data availability is still the limiting factor. If observations at critical time periods are lacking, the discrimination of certain crop types remains problematic. The classification errors that were related to inadequate remote sensing data (in terms of timing and coverage area) were strongly reduced with our post-classification methodology, but still led to additional spatial fragmentations of the crop sequence dataset. Also, a more rigorous generalization to reduce such fragments might not be the final solution. A significant increase in data availability is therefore expected though the Copernicus program of the European Union (EPC, 2014), which should further improve the results. We already started to integrate Sentinel-2, but also Sentinel-1 data into our approach (Lussem et al., 2016). Our first tests indicate that SAR classification results can be incorporated in the same way as optical remote sensing data.

Finally, concerning the ancillary data we used, similar dataset are available for many countries nowadays. Our Multi-Data Approach has sufficient degrees of freedom to integrate other geospatial data or other classifications methods like random forests (Belgiu and Drăguţ, 2016). Consequently, our approach is well suited to be transferred to other regions or countries.

Acknowledgments

The authors gratefully acknowledge financial support by the CRC/TR32 ‘Patterns in Soil-Vegetation-Atmosphere Systems: Monitoring, Modelling, and Data Assimilation’ funded by the German Research Foundation (DFG). We thank Geobasis.NRW for the provision of the ATKIS-Basic-DLM, the NASA Land Processes Distributed Active Archive Center (LP DAAC) for the provision of the ASTER data products and the US Geological Service (USGS) for the provision of the Landsat data products via the Earth Resources Observation and Science Center (EROS). Finally, we thank the Space Administration of the German Aerospace Center (DLR) and Planet Labs Germany GmbH for the provision of RapidEye data via the RapidEye Science Archive (RESA).

Appendix A. Supplementary data

Supplementary data associated with this article can be found, in the online version, at http://dx.doi.org/10.1016/j.jag.2017.04.009.

References

AdV, 2006. Documentation on the Modelling of Geoinformation of Official Surveying and

Mapping (GeoInfoDok) – Chapter 5 – Technical applications of the basic schema – Section 5.4 – Explanations on ATKIS®, Version 5.1, Status 31 July 2006. In: Afflerbach, S., Kunze, W. (Eds.), Working Committee of the Surveying Authorities of the States of the Federal Republic of Germany (AdV), pp. 74. http://www.adv-online.de/AAA-Modell/Dokumente-der-GeoInfoDok/binarywriterservlet?imgUid=8df46f15-1ff9-f216-afd6-ff3072e13d63&uBasVariant=11111111-1111-1111-1111-111111111111&isDownload=true (20.04.16).

Atzberger, C., 2013. Advances in remote sensing of agriculture: context description, existing operational monitoring systems and major information needs. Remote Sens. 5, 949–981.

Bareth, G., 2001. Integration einer IRS-1C-Landnutzungsklassifikation in das ATKIS zur Verbesserung der Information zur landwirtschaftlichen Nutzfläche am Beispiel des württembergischen Allgäus. GIS. Z. Raumbezogene Inf. Entscheid. 2001, 40–45.

Bareth, G., 2008. Multi-Data Approach (MDA) for Enhanced Land Use/Land Cover Mapping, The International Archives of the Photogrammetry, Remote Sensing and Spatial Information Sciences, vol. XXXVII. Part B8. Beijing 2008. International Society of the Photogrammetry and Remote Sensing Beijingpp. 1059–1066.

Bareth, G., 2009. GIS- and RS-based spatial decision support: structure of a spatial environmental information system (SEIS). Int. J. Digit. Earth 2, 134–154. http://dx.doi.org/10.1080/17538940902736315.

Bargiel, D., Herrmann, S., 2011. Multi-temporal land-cover classification of agricultural areas in two European regions with high resolution spotlight TerraSAR-X data. Remote Sens. 3, 859–877.

Belgiu, M., Drăguţ, L., 2016. Random forest in remote sensing: a review of applications and future directions. ISPRS J. Photogramm. Remote Sens. 114, 24–31. http://dx.doi.org/10.1016/j.isprsjprs.2016.01.011.

Blaes, X., Vanhalle, L., Defourny, P., 2005. Efficiency of crop identification based on optical and SAR image time series. Remote Sens. Environ. 96, 352–365. http://dx.doi.org/10.1016/j.rse.2005.03.010.

Blaschke, T., 2010. Object based image analysis for remote sensing. ISPRS J. Photogramm. Remote Sens. 65, 2–16.

BMELV, 2004. Verordnung über die Durchführung von Stützungsregelungen und des Integrierten Verwaltungs- und Kontrollsystems (InVeKoSVerordnung – InVeKoSV). Bundesministerium für Ernährung, Landwirtschaft und Verbraucherschutz. http://www.gesetze-im-internet.de/bundesrecht/invekosv/gesamt.pdf (04.10.12).

Boryan, C., Yang, Z., Mueller, R., Craig, M., 2011. Monitoring US agriculture: the US Department of Agriculture, National Agricultural Statistics Service, Cropland Data Layer Program. Geocarto Int. 26, 341–358. http://dx.doi.org/10.1080/10106049.2011.562309.

Boryan, C.G., Yang, Z., Willis, P., 2014. US geospatial crop frequency data layers. The Third International Conference on Agro-Geoinformatics, 11–14 August 2014. pp. 1–5. http://dx.doi.org/10.1109/Agro-Geoinformatics.2014.6910657.

Brisson, N., Gary, C., Justes, E., Roche, R., Mary, B., Ripoche, D., Zimmer, D., Sierra, J., Bertuzzi, P., Burger, P., Bussière, F., Cabidoche, Y.M., Cellier, P., Debaeke, P., Gaudillère, J.P., Hénault, C., Maraux, F., Seguin, B., Sinoquet, H., 2003. An overview of the crop model sticks. Eur. J. Agron. 18, 309–332. http://dx.doi.org/10.1016/S1161-0301(02)00110-7.

Campbell, J.B., Wynne, R.H., 2011. Introduction to Remote Sensing, 5th ed. The Guilford Press, New York.

Congalton, R.G., Green, K., 2009. Assessing the Accuracy of Remotely Sensed Data: Principles and Practices. CRC Press, Boca Raton.

Conrad, C., Fritsch, S., Zeidler, J., Rücker, G., Dech, S., 2010. Per-field irrigated crop classification in arid Central Asia using SPOT and ASTER data. Remote Sens. 2, 1035–1056.

Castellazzi, M.S., Wood, G.A., Burgess, P.J., Morris, J., Conrad, K.F., Perry, J.N., 2008. A systematic representation of crop rotations. Agric. Syst. 97, 26–33. http://dx.doi.org/10.1016/j.agsy.2007.10.006.

De Wit, A.J.W., Clevers, J.G.P.W., 2004. Efficiency and accuracy of per-field classification for operational crop mapping. Int. J. Remote Sens. 25, 4091–4112. http://dx.doi.org/10.1080/01431160310001619580.

Diepenbrock, W., Ellmer, F., Léon, J., 2012. Ackerbau, Pflanzenbau und Pflanzenzüchtung – Grundwissen Bachelor. UTB, Stuttgart.

Dingle Robertson, L., King, D.J., 2011. Comparison of pixel- and object-based classification in land cover change mapping. Int. J. Remote Sens. 32, 1505–1529. http://dx.doi.org/10.1080/01431160903571791.

Duro, D.C., Franklin, S.E., Dubé, M.G., 2012. A comparison of pixel-based and object-based image analysis with selected machine learning algorithms for the classification of agricultural landscapes using SPOT-5 HRG imagery. Remote Sens. Environ. 118, 259–272. http://dx.doi.org/10.1016/j.rse.2011.11.020.

EPC, 2014. Regulation (EU) No 377/2014 of the European Parliament and of the Council of 3 April 2014 Establishing the Copernicus Programme and Repealing Regulation (EU) No 911/2010, Official Journal of the European Union. European Parliament and Council. http://www.copernicus.eu/sites/default/files/library/Regulation_377_2014_Copernicus_3April2014.pdf (07.07.16).

ESRI, 2012a. Esri Grid Format, ArcGIS Desktop 10.0 Help. Environmental Systems Research Institute. http://help.arcgis.com/en/arcgisdesktop/10.0/help/index.html#//009t0000000w000000 (04.07.12).

ESRI, 2012b. Raster Dataset Attribute Tables, ArcGIS Desktop 10.0 Help. Environmental Systems Research Institute. http://help.arcgis.com/en/arcgisdesktop/10.0/help/index.html#/Raster_dataset_attribute_tables/009t00000009000000/ (04.07.12).

ESRI, 2016a. Calculate Field, ArcGIS Desktop 10.3 Help. http://desktop.arcgis.com/en/arcmap/10.3/tools/data-management-toolbox/calculate-field.htm (17.05.16).

ESRI, 2016b. Eliminate, ArcGIS Desktop 10.3 Help. http://desktop.arcgis.com/en/arcmap/10.3/tools/coverage-toolbox/eliminate.htm (10.05.16).

ESRI, 2016c. Union, ArcGIS Desktop 10.3 Help. http://desktop.arcgis.com/en/arcmap/10.3/tools/analysis-toolbox/union.htm (17.05.16).

ExelisVis, 2015a. Maximum Likelihood, ENVI 5.2 Help. Exelis Visual Information Solutions, Inc., Boulder, CO, USA.

ExelisVis, 2015b. Support Vector Machine, ENVI 5.2 Help. Exelis Visual Information Solutions, Inc., Boulder, CO, USA.

EU, 2009. Verordnung (EG) Nr 73/2009 des Rates vom 19. Januar 2009. Europäische Union. http://eur-lex.europa.eu/LexUriServ/LexUriServ.do?uri=OJ:L:2009:030:0016:0016:DE:PDF (04.10.12).

Foerster, S., Kaden, K., Foerster, M., Itzerott, S., 2012. Crop type mapping using spectral–temporal profiles and phenological information. Comput. Electron. Agric. 89, 30–40. http://dx.doi.org/10.1016/j.compag.2012.07.015.

Foody, G.M., Mathur, A., 2004. Toward intelligent training of supervised image classifications: directing training data acquisition for SVM classification. Remote Sens. Environ. 93, 107–117.

Foody, G.M., Mathur, A., 2006. The use of small training sets containing mixed pixels for accurate hard image classification: training on mixed spectral responses for classification by a SVM. Remote Sens. Environ. 103, 179–189.

Forkuor, G., Conrad, C., Thiel, M., Ullmann, T., Zoungrana, E., 2014. Integration of optical and Synthetic Aperture Radar imagery for improving crop mapping in Northwestern Benin, West Africa. Remote Sens. 6, 6472–6499.

Franklin, S.E., He, Y.H., Pape, A., Guo, X.L., McDermid, G.J., 2011. Landsat-comparable land cover maps using ASTER and SPOT images: a case study for large-area mapping programmes. Int. J. Remote Sens. 32, 2185–2205. http://dx.doi.org/10.1080/01431161003674642.

Gagliano, S., 2007. Include Classes. Exelis Visual Information Solutions, Inc., Boulder, CO, USA. http://www.exelisvis.com/Default.aspx?tabid=1540&id=1100 (17.01.13).

Geudtner, D., 2012. SENTINEL-1 System Overview and Performance. Earth Observing Missions and Sensors: Development, Implementation, and Characterization II 8528. http://dx.doi.org/10.1117/12.977485.

Giltrap, D.L., Li, C., Saggar, S., 2010. DNDC: a process-based model of greenhouse gas fluxes from agricultural soils. Agric. Ecosyst. Environ. 136, 292–300. http://dx.doi.org/10.1016/j.agee.2009.06.014.

Heywood, I., Cornelius, S., Carver, S., 2011. An Introduction to Geographical Information Systems, 4th ed. Prentice Hall, Harlow.

Hixson, M., Scholz, D., Fuhs, N., Akiyama, T., 1980. Evaluation of several schemes for classification of remotely sensed data. Photogramm. Eng. Remote Sens. 46, 1547–1553.

Huang, C., Davis, L.S., Townshend, J.R.G., 2002. An assessment of support vector machines for land cover classification. Int. J. Remote Sens. 23, 725–749.

Hütt, C., Koppe, W., Miao, Y., Bareth, G., 2016. Best accuracy land use/land cover (LULC) classification to derive crop types using multitemporal, multisensor, and multi-polarization SAR satellite images. Remote Sens. 8, 684.

Immitzer, M., Vuolo, F., Atzberger, C., 2016. First experience with Sentinel-2 data for crop and tree species classifications in Central Europe. Remote Sens. 8, 166.

IT.NRW, 2009. Agrarstrukturerhebung in Nordrhein-Westfalen 2007 – Gemeinde- und Kreisstatistik der landwirtschaftlichen Betriebe – Betriebsgrößen, Bodennutzung und Viehhaltung; sozialökonomische Betriebstypen und betriebswirtschaftliche Ausrichtung; Arbeitskräfte. Information und Technik Nordrhein-Westfalen (Geschäftsbereich Statistik), Düsseldorf, pp. 259. https://webshop.it.nrw.de/gratis/C969%20200751.pdf (25.10.13).

IT.NRW, 2012. Landwirtschaftszählung in Nordrhein-Westfalen 2010 – Gemeinde- und Kreisstatistik der landwirtschaftlichen Betriebe Betriebsgrößen, Bodennutzung, Viehhaltung, sozialökonomische Betriebstypen, betriebswirtschaftliche Ausrichtung, Arbeitskräfte. Information und Technik Nordrhein-Westfalen (Geschäftsbereich Statistik), Düsseldorf, pp. 266. https://webshop.it.nrw.de/gratis/C919%20201051.pdf (25.10.13).

Jensen, J.R., 2016. Introductory Digital Image Processing: A Remote Sensing Perspective, 4th ed. Pearson, Upper Saddle River.

Kappas, M., 2011. Geographische Informationssysteme. Westermann, Braunschweig.

KBTL, 2009. Faustzahlen für die Landwirtschaft, 14 ed. Kuratorium für Technik und Bauwesen in der Landwirtschaft e.V., Darmstadt.

Kersebaum, K.C., Hecker, J.-M., Mirschel, W., Wegehenkel, M., 2007. Modelling water and nutrient dynamics in soil–crop systems: a comparison of simulation models applied on common data sets. In: Kersebaum, K.C., Hecker, J.-M., Mirschel, W., Wegehenkel, M. (Eds.), Modelling Water and Nutrient Dynamics in Soil–Crop Systems. Springer, Dortrecht, pp. 1–17.

Klöcking, B., Ströbl, B., Knoblauch, S., Maier, U., Pfützner, B., Gericke, A., 2003. Development and allocation of land-use scenarios in agriculture for hydrological impact studies. Phys. Chem. Earth, Parts A/B/C 28, 1311–1321. http://dx.doi.org/10.1016/j.pce.2003.09.007.

Koppe, W., Gnyp, M.L., Hütt, C., Yao, Y., Miao, Y., Chen, X., Bareth, G., 2013. Rice monitoring with multi-temporal and dual-polarimetric TerraSAR-X data. Int. J. Appl. Earth Obs. Geoinf. 21, 568–576. http://dx.doi.org/10.1016/j.jag.2012.07.016.

Lenz-Wiedemann, V.I.S., Klar, C.W., Schneider, K., 2010. Development and test of a crop growth model for application within a Global Change decision support system. Ecol. Model. 221, 314–329. http://dx.doi.org/10.1016/j.ecolmodel.2009.10.014.

Leteinturier, B., Herman, J.L., Longueville, F.d., Quintin, L., Oger, R., 2006. Adaptation of a crop sequence indicator based on a land parcel management system. Agric. Ecosyst. Environ. 112, 324–334. http://dx.doi.org/10.1016/j.agee.2005.07.011.

Li, Q., Wang, C., Zhang, B., Lu, L., 2015. Object-based crop classification with Landsat-MODIS enhanced time-series data. Remote Sens. 7, 15820.

Lobell, D.B., Thau, D., Seifert, C., Engle, E., Little, B., 2015. A scalable satellite-based crop yield mapper. Remote Sens. Environ. 164, 324–333. http://dx.doi.org/10.1016/j.rse.2015.04.021.

Long, J.A., Lawrence, R.L., Greenwood, M.C., Marshall, L., Miller, P.R., 2013. Object-oriented crop classification using multitemporal ETM+ SLC-off imagery and random forest. GISci. Remote Sens. 50, 418–436. http://dx.doi.org/10.1080/15481603.2013.

817150.
Lorenz, M., Fürst, C., Thiel, E., 2013. A methodological approach for deriving regional crop rotations as basis for the assessment of the impact of agricultural strategies using soil erosion as example. J. Environ. Manag. 127 (Supplement), S37–S47. http://dx.doi.org/10.1016/j.jenvman.2013.04.050.
Löw, F., Conrad, C., Michel, U., 2015. Decision fusion and non-parametric classifiers for land use mapping using multi-temporal RapidEye data. ISPRS J. Photogramm. Remote Sens. 108, 191–204. http://dx.doi.org/10.1016/j.isprsjprs.2015.07.001.
Lucas, R., Medcalf, K., Brown, A., Bunting, P., Breyer, J., Clewley, D., Keyworth, S., Blackmore, P., 2011. Updating the Phase 1 habitat map of Wales, UK, using satellite sensor data. ISPRS J. Photogramm. Remote Sens. 66, 81–102.
Lussem, U., Waldhoff, G., 2013a. Enhanced Land Use Classification of 2011 for the Rur Catchment. http://dx.doi.org/10.5880/TR32DB.7.
Lussem, U., Waldhoff, G., 2013b. Land Use Classification 2012 of the Rur Catchment. CRC/TR32 Database (TR32DB). http://dx.doi.org/10.5880/TR32DB.9.
Lussem, U., Waldhoff, G., 2014. Enhanced Land Use Classification 2013 of the Rur Catchment. CRC/TR32 Database (TR32DB). http://dx.doi.org/10.5880/TR32DB.11.
Lussem, U., Waldhoff, G., 2015. Enhanced Land Use Classification 2014 of the Rur Catchment – Update. CRC/TR32 Database (TR32DB). http://dx.doi.org/10.5880/TR32DB.13.
Lussem, U., Hütt, C., Waldhoff, G., 2016. Combined analysis of sentinel-1 and rapideye data for improved crop type classification: an early season approach for rapeseed and cereals. Int. Arch. Photogramm. Remote Sens. Spatial Inf. Sci. XLI-B8 959–963. http://dx.doi.org/10.5194/isprs-archives-XLI-B8-959-2016.
LWK-NRW, 2008. Getreide: Saatzeiten und Saatstärken – Ratgeber 2008. Landwirtschaftskammer Nordrhein-Westfalen, Bonn. http://www.landwirtschaftskammer.de/landwirtschaft/ackerbau/getreide/getreide-saatstaerken-pdf.pdf (12.06.08).
LWK NRW, 2005. Feldblöcke. Landwirtschaftskammer Nordrhein-Westfalen, Bonn. http://www.landwirtschaftskammer.de/foerderung/feldblock/index.htm, XXXXX.
LWK NRW, 2011. LZ Rheinland – Ratgeber Förderung 2011. Landwirtschaftskammer Nordrhein-Westfalen, Bonn. http://www.landwirtschaftskammer.de/foerderung/pdf/ratgeber-foerderung-2011.pdf (12.01.12).
LWK NRW, 2012. Fruchtfolge – Ratgeber 2012. Landwirtschaftskammer Nordrhein-Westfalen, Bonn, Münster. http://www.landwirtschaftskammer.de/landwirtschaft/ackerbau/fruchtfolge/tabellen-fruchtfolge-pdf.pdf (26.11.13).
Mathur, A., Foody, G.M., 2008. Crop classification by support vector machine with intelligently selected training data for an operational application. Int. J. Remote Sens. 29, 2227–2240. http://dx.doi.org/10.1080/01431160701395203.
McNairn, H., Champagne, C., Shang, J., Holmstrom, D., Reichert, G., 2009. Integration of optical and Synthetic Aperture Radar (SAR) imagery for delivering operational annual crop inventories. ISPRS J. Photogramm. Remote Sens. 64, 434–449. http://dx.doi.org/10.1016/j.isprsjprs.2008.07.006.
McNairn, H., Kross, A., Lapen, D., Caves, R., Shang, J., 2014. Early season monitoring of corn and soybeans with TerraSAR-X and RADARSAT-2. Int. J. Appl. Earth Obs. Geoinf. 28, 252–259. http://dx.doi.org/10.1016/j.jag.2013.12.015.
Meier, U., 2001. Entwicklungsstadien mono- und dikotyler Pflanzen – BBCH Monografie. Biologische Bundesanstalt für Land und Forstwirtschaft. pp. 165. http://www.jki.bund.de/fileadmin/dam_uploads/_veroeff/bbch/BBCH-Skala_deutsch.pdf (10.01.13).
Mountrakis, G., Im, J., Ogole, C., 2011. Support vector machines in remote sensing: a review. ISPRS J. Photogramm. Remote Sens. 66, 247–259.
Mulla, D.J., 2013. Twenty five years of remote sensing in precision agriculture: key advances and remaining knowledge gaps. Biosyst. Eng. 114, 358–371. http://dx.doi.org/10.1016/j.biosystemseng.2012.08.009.
Munzert, M., 2006. Pflanzliche Erzeugung – Die Landwirtschaft. BLV Buchverlag GmbH & Co, KG, München.
Nendel, C., Berg, M., Kersebaum, K.C., Mirschel, W., Specka, X., Wegehenkel, M., Wenkel, K.O., Wieland, R., 2011. The MONICA model: testing predictability for crop growth, soil moisture and nitrogen dynamics. Ecol. Model. 222, 1614–1625. http://dx.doi.org/10.1016/j.ecolmodel.2011.02.018.
Oetter, D.R., Cohen, W.B., Berterretche, M., Maiersperger, T.K., Kennedy, R.E., 2000. Land cover mapping in an agricultural setting using multiseasonal Thematic Mapper data. Remote Sens. Environ. 76, 139–155. http://dx.doi.org/10.1016/S0034-4257(00)00202-9.
Pax-Lenney, M., Woodcock, C.E., 1997. Monitoring agricultural lands in Egypt with multitemporal landsat TM imagery: how many images are needed? Remote Sens. Environ. 59, 522–529. http://dx.doi.org/10.1016/S0034-4257(96)00124-1.
Peña-Barragán, J.M., Ngugi, M.K., Plant, R.E., Six, J., 2011. Object-based crop identification using multiple vegetation indices, textural features and crop phenology. Remote Sens. Environ. 115, 1301–1316. http://dx.doi.org/10.1016/j.rse.2011.01.009.
Peña, J., Gutiérrez, P., Hervás-Martínez, C., Six, J., Plant, R., López-Granados, F., 2014. Object-based image classification of summer crops with machine learning methods. Remote Sens. 6, 5019.
Resop, J.P., Fleisher, D.H., Wang, Q., Timlin, D.J., Reddy, V.R., 2012. Combining explanatory crop models with geospatial data for regional analyses of crop yield using field-scale modeling units. Comput. Electron. Agric. 89, 51–61. http://dx.doi.org/10.1016/j.compag.2012.08.001.
Richards, J.A., 2012. Remote Sensing Digital Image Analysis: An Introduction, 5th ed. Springer, Berlin Heidelberg.
Rohierse, A., Bareth, G., 2004. Integration einer multitemporalen Satellitenbildklassifikation in ATKIS zur weiteren Differenzierung der Objektart Ackerland. GIS 2004, 35–41.
Rounsevell, M.D.A., Annetts, J.E., Audsley, E., Mayr, T., Reginster, I., 2003. Modelling the spatial distribution of agricultural land use at the regional scale. Agric. Ecosyst. Environ. 95, 465–479. http://dx.doi.org/10.1016/S0167-8809(02)00217-7.
Roy, P.S., Behera, M.D., Murthy, M.S.R., Roy, A., Singh, S., Kushwaha, S.P.S., Jha, C.S., Sudhakar, S., Joshi, P.K., Reddy, C.S., Gupta, S., Pujar, G., Dutt, C.B.S., Srivastava, V.K., Porwal, M.C., Tripathi, P., Singh, J.S., Chitale, V., Skidmore, A.K., et al., 2015. New vegetation type map of India prepared using satellite remote sensing: comparison with global vegetation maps and utilities. Int. J. Appl. Earth Obs. Geoinf. 39, 142–159. http://dx.doi.org/10.1016/j.jag.2015.03.003.
Schneider, K., 2003. Assimilating remote sensing data into a land-surface process model. Int. J. Remote Sens. 24, 2959–2980. http://dx.doi.org/10.1080/01431160210154803.
Schönhart, M., Schmid, E., Schneider, U.A., 2011. CropRota – a crop rotation model to support integrated land use assessments. Eur. J. Agron. 34, 263–277. http://dx.doi.org/10.1016/j.eja.2011.02.004.
Siachalou, S., Mallinis, G., Tsakiri-Strati, M., 2015. A hidden Markov models approach for crop classification: linking crop phenology to time series of multi-sensor remote sensing data. Remote Sens. 7, 3633.
Smith, G.M., Fuller, R.M., 2001. An integrated approach to land cover classification: an example in the Island of Jersey. Int. J. Remote Sens. 22, 3123–3142. http://dx.doi.org/10.1080/01431160152558288.
Song, C., Woodcock, C.E., Seto, K.C., Lenney, M.P., Macomber, S.A., 2001. Classification and change detection using Landsat TM data: when and how to correct atmospheric effects? Remote Sens. Environ. 75, 230–244.
Teluguntla, P.G., Thenkabail, P.S., Xiong, J.N., Gumma, M.K., Giri, C., Milesi, C., Ozdogan, M., Congalton, R., Tilton, J., Sankey, T.T., Massey, R., Phalke, A., Yadav, K., 2015. Global Cropland Area Database (GCAD) Derived from Remote Sensing in Support of Food Security in the Twenty-First Century: Current Achievements and Future Possibilities, Land Resources Monitoring, Modeling, and Mapping with Remote Sensing (Remote Sensing Handbook). Taylor & Francis, Boca Raton, Florida.
Thenkabail, P.S., 2010. Global croplands and their importance for water and food security in the twenty-first century: towards an ever green revolution that combines a second green revolution with a blue revolution. Remote Sens. 2, 2305–2312.
Thenkabail, P.S., 2012. Global croplands and their water use for food security in the twenty-first century foreword. Photogramm. Eng. Remote Sens. 78, 797–798.
Turker, M., Arikan, M., 2005. Sequential masking classification of multi-temporal Landsat7 ETM+ images for field based crop mapping in Karacabey, Turkey. Int. J. Remote Sens. 26, 3813–3830. http://dx.doi.org/10.1080/01431160500166391.
Van Niel, T.G., McVicar, T.R., 2004. Determining temporal windows for crop discrimination with remote sensing: a case study in south-eastern Australia. Comput. Electron. Agric. 45, 91–108. http://dx.doi.org/10.1016/j.compag.2004.06.003.
van Wart, J., Kersebaum, K.C., Peng, S., Milner, M., Cassman, K.G., 2013. Estimating crop yield potential at regional to national scales. Field Crops Res. 143, 34–43. http://dx.doi.org/10.1016/j.fcr.2012.11.018.
Vapnik, V.N., 1995. The Nature of Statistical Learning Theory. Springer, New York.
Waldhoff, G., 2012a. Enhanced Land Use Classification of 2008 for the Rur Catchment. CRC/TR32 Database (TR32DB). http://dx.doi.org/10.5880/TR32DB.7.
Waldhoff, G., 2012b. Enhanced Land Use Classification of 2009 for the Rur Catchment. CRC/TR32 Database (TR32DB). http://dx.doi.org/10.5880/TR32DB.2.
Waldhoff, G., 2012c. Enhanced Land Use Classification of 2010 for the Rur Catchment. CRC/TR32 Database (TR32DB). http://dx.doi.org/10.5880/TR32DB.3.
Waldhoff, G., Bareth, G., 2009. GIS- and RS-based land use and land cover analysis: case study Rur-Watershed, Germany, Geoinformatics 2008 and joint conference on GIS and built environment: advanced spatial data models and analyses. Proc. SPIE 7146. SPIEpp. 714626–714628. http://dx.doi.org/10.1117/12.813171.
Waldhoff, G., Curdt, C., Hoffmeister, D., Bareth, G., 2012. Analysis of multitemporal and multisensor remote sensing data for crop rotation mapping. ISPRS Ann. Photogramm. Remote Sens. Spat. Inf. Sci. I-7, 177–182. http://dx.doi.org/10.5194/isprsannals-I-7-177-2012.
Waldhoff, G., Lussem, U., 2016. Enhanced Land Use Classification 2015 of the Rur Catchment – Update. CRC/TR32 Database (TR32DB). http://dx.doi.org/10.5880/TR32DB.19.
Waldner, F., Canto, G.S., Defourny, P., 2015. Automated annual cropland mapping using knowledge-based temporal features. ISPRS J. Photogramm. Remote Sens. 110, 1–13. http://dx.doi.org/10.1016/j.isprsjprs.2015.09.013.
Wardlow, B.D., Egbert, S.L., Kastens, J.H., 2007. Analysis of time-series MODIS 250 m vegetation index data for crop classification in the U.S. Central Great Plains. Remote Sens. Environ. 108, 290–310. http://dx.doi.org/10.1016/j.rse.2006.11.021.
Whitcraft, A.K., Vermote, E.F., Becker-Reshef, I., Justice, C.O., 2015. Cloud cover throughout the agricultural growing season: impacts on passive optical earth observations. Remote Sens. Environ. 156, 438–447. http://dx.doi.org/10.1016/j.rse.2014.10.009.
Wilson, H.M., Al-Kaisi, M.M., 2008. Crop rotation and nitrogen fertilization effect on soil CO_2 emissions in central Iowa. Appl. Soil Ecol. 39, 264–270. http://dx.doi.org/10.1016/j.apsoil.2007.12.013.
Wu, B., Gommes, R., Zhang, M., Zeng, H., Yan, N., Zou, W., Zheng, Y., Zhang, N., Chang, S., Xing, Q., van Heijden, A., 2015. Global crop monitoring: a satellite-based hierarchical approach. Remote Sens. 7, 3907.
Zheng, B., Myint, S.W., Thenkabail, P.S., Aggarwal, R.M., 2015. A support vector machine to identify irrigated crop types using time-series Landsat NDVI data. Int. J. Appl. Earth Obs. Geoinf. 34, 103–112. http://dx.doi.org/10.1016/j.jag.2014.07.002.